

A Decade of Deep Learning for Remote Sensing Spatiotemporal Fusion: Advances, Challenges, and Opportunities

Enzhe Sun^a, Yongchuan Cui^{b,c}, Peng Liu^{b,c,*} and Jining Yan^{a,*}

^aSchool of Computer Science, China University of Geosciences (Wuhan), Wuhan 430078, China

^bAerospace Information Research Institute, Chinese Academy of Sciences, Beijing 100094, China

^cSchool of Electronic, Electrical and Communication Engineering, University of Chinese Academy of Sciences, Beijing 101408, China

ARTICLE INFO

Keywords:

Spatiotemporal fusion

Deep learning

Remote sensing

Literature review

ABSTRACT

Hardware limitations and satellite launch costs make direct acquisition of high temporal-spatial resolution remote sensing imagery challenging. Remote sensing spatiotemporal fusion (STF) technology addresses this problem by merging high temporal but low spatial resolution imagery with high spatial but low temporal resolution imagery to efficiently generate high spatiotemporal resolution satellite images. STF provides unprecedented observational capabilities for land surface change monitoring, agricultural management, and environmental research. Deep learning (DL) methods have revolutionized the remote sensing spatiotemporal fusion field over the past decade through powerful automatic feature extraction and nonlinear modeling capabilities, significantly outperforming traditional methods in handling complex spatiotemporal data. Despite the rapid development of DL-based remote sensing STF, the community lacks a systematic review of this quickly evolving field. This paper comprehensively reviews DL developments in remote sensing STF over the last decade, analyzing key research trends, method classifications, commonly used datasets, and evaluation metrics. It discusses major challenges in existing research and identifies promising future research directions as references for researchers in this field to inspire new ideas. The specific models, datasets, and other information mentioned in this article have been collected in: <https://github.com/yc-cui/Deep-Learning-Spatiotemporal-Fusion-Survey>.

1. Introduction

Spatiotemporal fusion (STF) is a fundamental technique that integrates data with different spatial and temporal resolutions to generate high-quality imagery with enhanced spatiotemporal characteristics. As a broadly applicable method, STF has demonstrated its versatility across various fields. In computer vision (CV), STF plays a crucial role in video analysis and action recognition by effectively merging temporal and spatial information to better understand dynamic changes in visual data [1]. In urban planning and traffic management, STF enables the integration of traffic flow data from different temporal and spatial scales, facilitating more accurate congestion prediction and optimization of urban traffic systems [2]. The medical field also benefits from STF through its application in medical imaging analysis, where it facilitates the visualization of dynamic processes such as tumor growth and disease progression by fusing images from different time points (*e.g.*, CT and MRI scans) [3].

In the context of remote sensing (RS), STF has emerged as a particularly valuable technique for addressing the inherent trade-off between spatial and temporal resolution in Earth observation (EO). As illustrated in Figure 1, the core challenge in remote sensing STF lies in effectively combining high temporal but low spatial resolution (HTLS) data with high spatial but low temporal resolution (HSLT) data to generate synthetic imagery that maintains both high spatial and temporal characteristics [4]. This capability is crucial

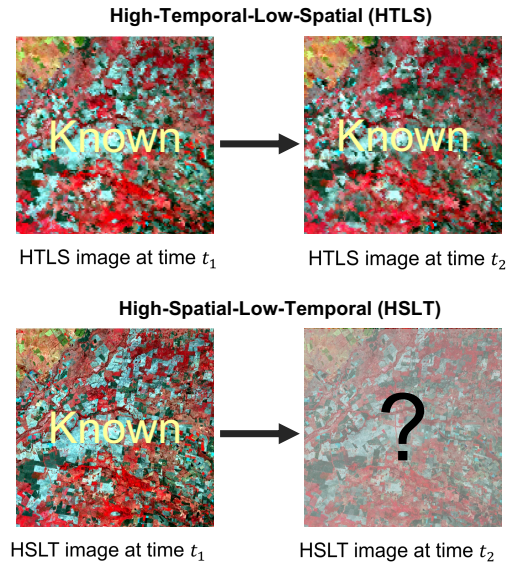


Figure 1: Fusion of remote sensing images.

for various Earth observation applications, including land surface monitoring, environmental research, and agricultural management, *etc.*

The contradiction in STF is a major challenge due to the difference in spatial and temporal dimensions [5]. HTLS images from sensors such as Moderate Resolution Imaging Spectroradiometer (MODIS), for example, provide frequent temporal snapshots at the expense of reduced spatial resolution. In contrast, HSLT imagery, which offers detailed

*Corresponding author

✉senzhe1113@hotmail.com (E. Sun); cugcuiyc@cug.edu.cn (Y. Cui);

liupeng202303@aircas.ac.cn (P. Liu); yanjn@cug.edu.cn (J. Yan)

ORCID(s): 0000-0003-3292-8551 (P. Liu); 0000-0003-0680-5427 (J. Yan)

spatial information in the form of high resolution, has limited temporal information due to fewer time updates. Due to this inherent contradiction, generating fused products that maintain both high temporal and spatial resolution presents significant challenges [6, 7]. As illustrated in Figure 1, spatiotemporal fusion techniques enable HTLS and HSLT to work together, combining these two types of data to produce enhanced products that capitalize on the strengths of both input sources, thus improving overall performance.

Traditional STF methods can be systematically classified based on their underlying mathematical modeling principles [5, 8], which fall into five main categories:

Bayesian-based methods. Bayesian estimation of information serves as a method for probabilistic image analysis [6, 9]. Some of the most well-known approaches include Bayesian Maximum Entropy (BME) [10] and the unified fusion model [11]. The Bayesian approaches are particularly useful in the dynamic and complex situations of environmental analysis such as vegetation and climate change monitoring. These methods are valuable in the field of image noise reduction and can be effectively applied to complex environmental scenarios requiring detailed situational awareness [12, 13].

Unmixing-based methods. These methods estimate the high-resolution pixel values by decomposing low-resolution pixels into endmembers based on linear spectral mixing theory [13, 14, 15]. Well-known models include MMT (Multiresolution Spectral-Matching Technique) [16] and others. Although they are limited by the linear assumptions in heterogeneous areas, these approaches are useful for sub-pixel analysis, especially in multisource remote sensing data fusion [9, 12, 17].

Learning-based methods. These methods aim to represent the relationship between coarse and fine resolution images, predicting the final high-resolution image based on patterns learned from previous observations [18]. Learning-based approaches establish models that simulate the relationship between images of different resolutions, capturing features that may not be directly observed in the final images. These methods can effectively process images with similar characteristics to those in the training set, automatically extracting features from large datasets [19].

Weight function-based methods. These methods estimate high-resolution pixel values by combining information from multiple input images using weighted functions. Prominent techniques include STARFM (Spatial and Temporal Adaptive Reflectance Fusion Model) [20], ESTARFM (Enhanced STARFM) [21], STAARCH (Spatiotemporal Adaptive Reflectance Correction for High-Resolution RS Images) [22], and others. These methods perform well in homogeneous areas but are less effective when dealing with nonlinear changes or complex terrain [6, 13].

Hybrid methods. Hybrid methods enhance fusion performance by integrating advantages from different techniques. For example, FSDAF [23] combines the strengths of unmixing and weight function approaches to process complex spatiotemporal data, significantly improving fusion accuracy

and environmental adaptability, especially suitable for high-resolution RS image processing scenarios [9, 12].

The application of deep learning (DL) technology in RS STF research has attracted considerable attention in recent years, a trend arising from the rapid coordinated development of RS technology and DL methods [23]. Compared to traditional methods, DL offers distinct advantages in feature extraction, non-linear modeling, and data adaptability. While traditional methods often rely on manually designed features and assume simple surface change patterns [16, 24, 25], DL can automatically extract multi-level spatiotemporal features through large-scale data training, effectively solving non-linear relationship problems in complex scenarios. DL methods have higher tolerance for data noise and missing information, generating more stable fusion images and better adapting to multi-source, multi-modal RS data fusion requirements. These characteristics make deep learning a key driving force in the development of spatiotemporal fusion technology [26, 27].

This paper systematically reviews the application of deep learning in remote sensing spatiotemporal fusion over the past decade, highlighting the unique advantages and development potential of deep learning methods while analyzing current technical limitations and future development directions. Figure 2 provides a visual framework illustrating this survey's structure.

1.1. Analysis of Research Trends of DL for RS STF

To visually demonstrate research trends and scope, we conducted statistical analysis of relevant literature in the Web of Science (WOS) database, collecting data on different research methods through two advanced searches, providing data support for exploring the evolution and future development trends in this field. Query Q1 was used to filter literature closely related to *deep learning*, *remote sensing*, and *spatiotemporal fusion* with the specific search topic: (TS=remote sensing) AND (TS=spatiotemporal fusion) AND (TS=deep learning). Query Q2 was broader and not limited to deep learning methods: (TS=remote sensing) AND (TS=spatiotemporal fusion). For clarity, in the WOS database, TS refers to topic search, which searches for specified terms in titles, abstracts, author keywords, and keywords plus. Based on these two queries, we selected recent literature on these topics and conducted visualization analysis (see Table 1 and Figure 3).

Figure 3 shows that the cumulative number of Q1 literature increased from 1 article in 2017 to 121 articles in 2024, with the ratio of Q1 to Q2 rising from 0.06 to 0.25. This indicates a significant growth in the proportion of deep learning methods in the spatiotemporal fusion field over the past eight years, highlighting its emergence as an important research direction in this domain.

To gain a more comprehensive understanding of research hotspots in DL for STF, we also generated a keyword word cloud using the all collected literatures, as shown in Figure 4, from which high-frequency keywords and their distribution

Table 1
Web of Science data retrieval results (2017-2024).

Query	Topic	Results
Q1	(TS=remote sensing) AND (TS=spatiotemporal fusion) AND (TS=deep learning)	121
Q2	(TS=remote sensing) AND (TS=spatiotemporal fusion)	509

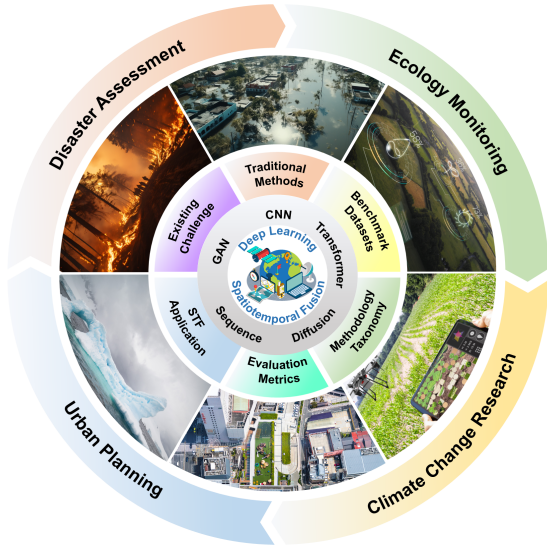


Figure 2: Overview of DL-based RS STF framework and applications. This figure illustrates the comprehensive landscape covered in this review, including: (a) the network architectures examined (CNN, Transformer, GAN, Diffusion, and sequence models, etc.); (b) the thematic progression of the paper sections from analysis of research trends to future opportunities; (c) key application domains of STF technologies; and (d) visual representations of the methodological framework. This graphical abstract serves as a roadmap for understanding the decade-long evolution of deep learning approaches in remote sensing spatiotemporal fusion discussed throughout the paper.

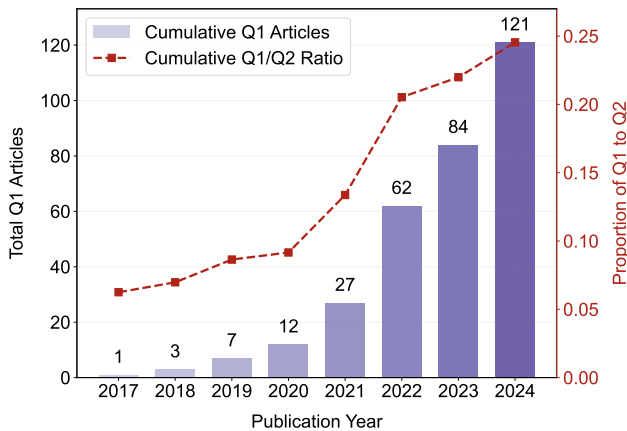


Figure 3: Number of published articles annually in Q1 and its proportion on Q2.

characteristics can be observed. The word cloud shows *Land-sat* and *MODIS* as the most commonly used remote sensing data sources, highlighting their core role in STF research. The frequent appearance of deep learning-related technical terms underscores their importance in spatiotemporal fusion. *Deep* and *Models* reflect the widespread application of deep learning models in this field, while *Convolutional* and *GAN* demonstrate the application trends of convolutional neural networks [28] and generative adversarial networks [29, 30]. In recent years, attention mechanisms and Transformer [31] models have gradually become new trends in STF research, as evidenced by related words like *Attention* and *Transformer*. Additionally, the word cloud highlights key research areas related to remote sensing image features, such as *Spectral* and *Pixels*, emphasizing the importance of multispectral features and pixel-level processing, while *Land* and *Vegetation* reflect research directions in STF concerning land cover and ecological monitoring. This word cloud demonstrates the extensive application of deep learning in spatiotemporal fusion and the rapid development of emerging technologies, clearly outlining the research framework and key directions in this field.

1.2. Previous Surveys and Scope

Previous surveys has played an important role in summarizing basic knowledge, technological developments, and typical applications in the remote sensing STF field [6]. However, most reviews primarily focus on traditional spatiotemporal fusion methods and have not comprehensively covered the latest advances in deep learning for remote sensing spatiotemporal fusion [26].

Previous reviews have summarized and classified different techniques in remote sensing spatiotemporal fusion. Zhu *et al.* [32] systematically reviewed spatiotemporal fusion methods for multi-source remote sensing data and proposed a classification framework including several major categories such as regression methods, dictionary learning methods, and physical model methods, but did not deeply explore the potential of deep learning methods. Li *et al.* [12] focused on spatiotemporal fusion techniques for remote sensing data and conducted experimental comparisons of different models, but mainly concentrated on traditional machine learning methods, lacking detailed analysis of deep learning models that have emerged in recent years. Belgiu and Stein [6] mentioned some studies using neural networks but did not conduct in-depth analysis of these models' structures, data requirements, and application scenarios.

Despite covering different techniques and application scenarios of spatiotemporal fusion, existing reviews still have

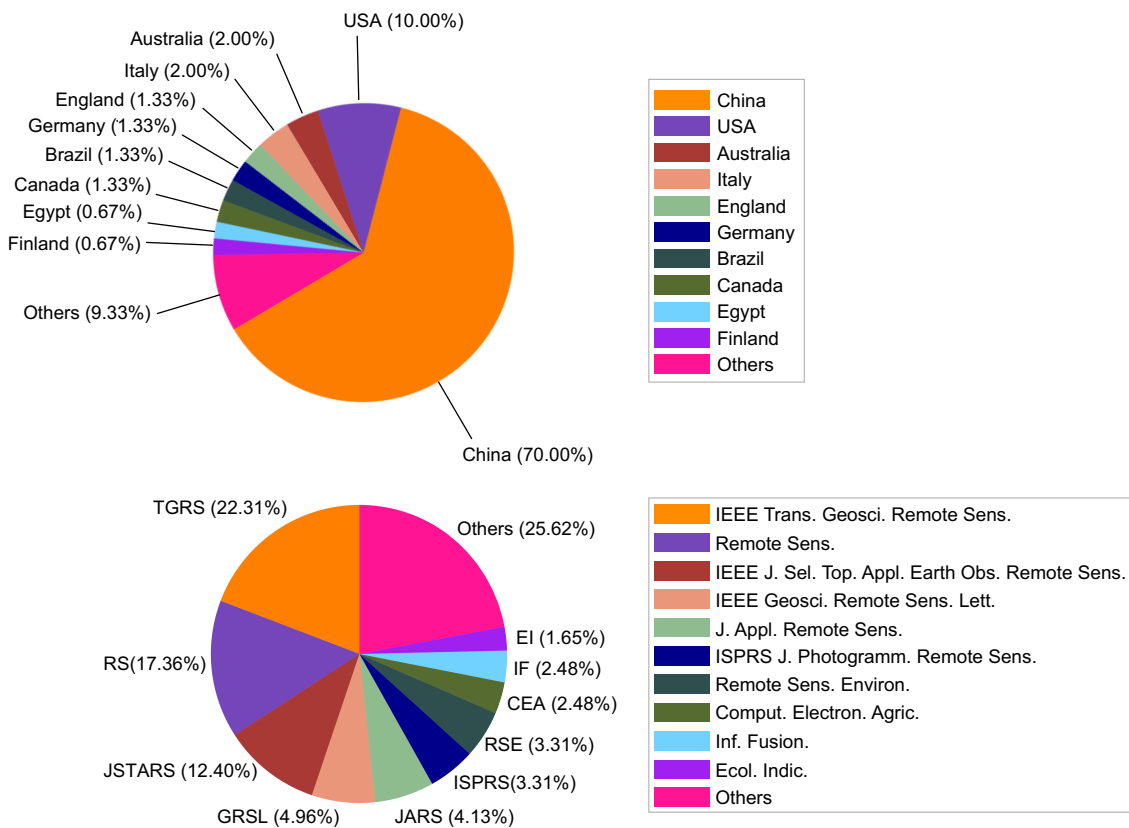


Figure 6: Distribution of published articles by top countries and journals.

2.2. Benchmark Datasets

Benchmark datasets play a crucial role in remote sensing spatiotemporal fusion research, providing unified standards for model training, evaluation, and performance comparison that are essential for assessing deep learning algorithms and promoting technological advancement [34, 35, 36]. After more than a decade of development, a relatively complete dataset system has been established [37], as summarized in Table 3.

These datasets display a clear hierarchical structure when viewed from their spatiotemporal characteristics [38, 39]. Terrestrial observation datasets typically employ complementary configurations of *high spatial - low temporal* resolution (e.g., Landsat’s 30m/16 days) and *low spatial - high temporal* resolution (e.g., MODIS’s 500m/1 day), creating standardized frameworks for evaluating the spatiotemporal reconstruction capabilities of fusion algorithms. In contrast, oceanic observation datasets (e.g., GOCI-II) offer unique high temporal resolution (1 hour) [40, 41]. As shown in Figure 7, the spatial distribution of existing benchmark datasets exhibits notable regional clustering, primarily concentrated in Asia and Oceania. The figure also presents image comparisons between Landsat and MODIS for five representative datasets (CIA, LGC, AHB, Tianjin, and Daxing), as well as between Gaofen and Landsat for the Wuhan dataset, collectively covering six distinct geographical regions.

The distribution of research areas within these datasets encompasses various typical geographical scenario [42]. In China, the AHB dataset records surface change processes in Inner Mongolia’s Ar Horqin Banner region, which has unique geographical and climatic conditions, providing an excellent platform for validating fusion data performance in heterogeneous areas [12]. The Tianjin dataset captures dynamic change characteristics in a rapidly urbanizing region, with 27 data pairs comprehensively documenting urban expansion and seasonal variations. The Daxing dataset records the entire construction process of Beijing Daxing International Airport from 2013 to 2019, including dramatic land cover changes that reflect related changes in surrounding areas [43]. The CIA and LGC datasets focus on agricultural areas in Australia, covering the Coleambally Irrigation Area and Lower Gwydir Catchment [44, 45]. Their surface changes primarily reflect cyclical patterns of irrigation agricultural activities, offering ideal benchmarks for evaluating the performance of spatiotemporal fusion methods [26, 46].

2.3. Methodology Taxonomy

The introduction of deep learning technology in the research of remote sensing spatiotemporal fusion has significantly enhanced the models’ ability to model complex spatiotemporal features [55, 56]. Based on network architecture and technical characteristics, existing methods can be classified into the following categories: Convolutional

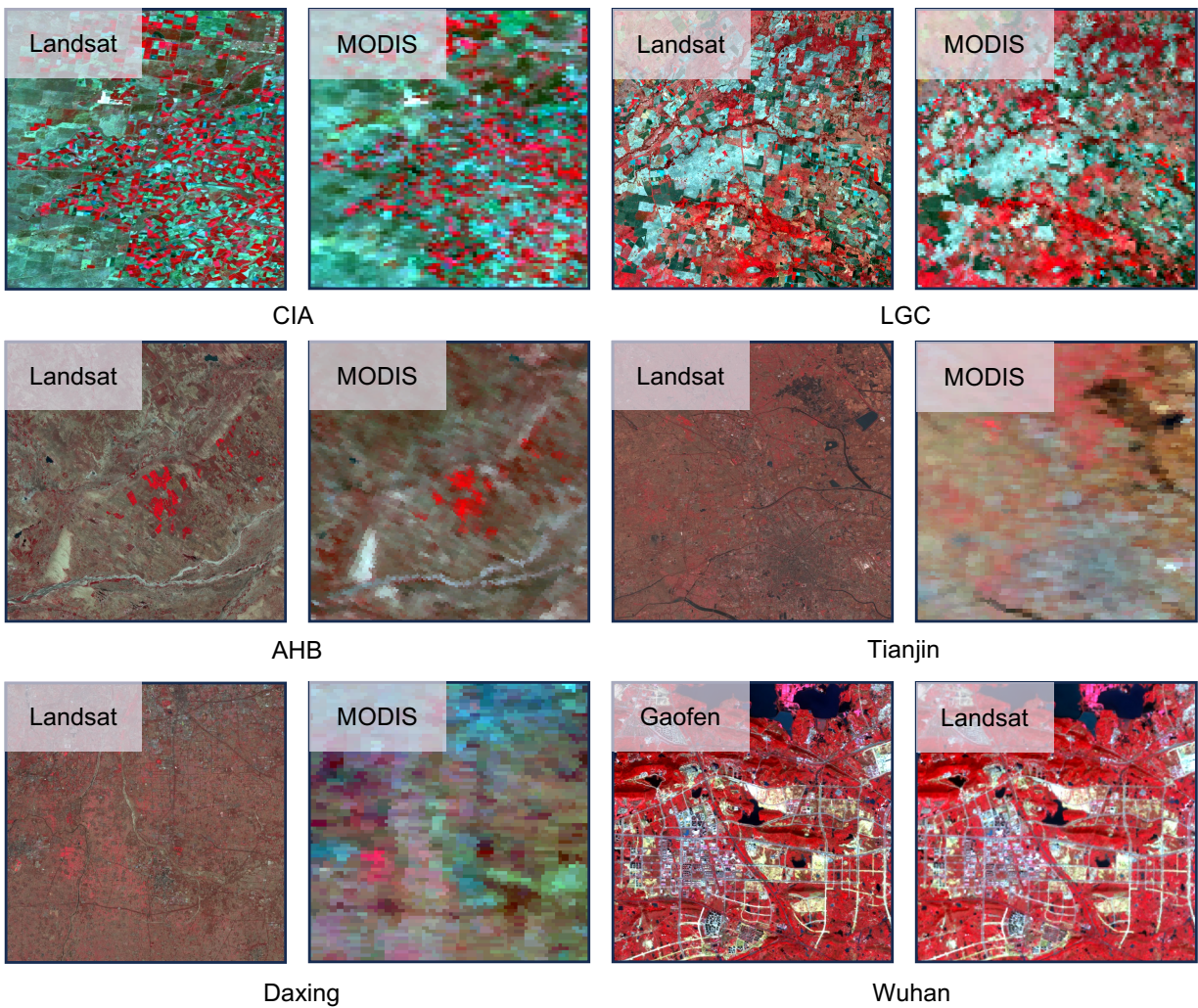
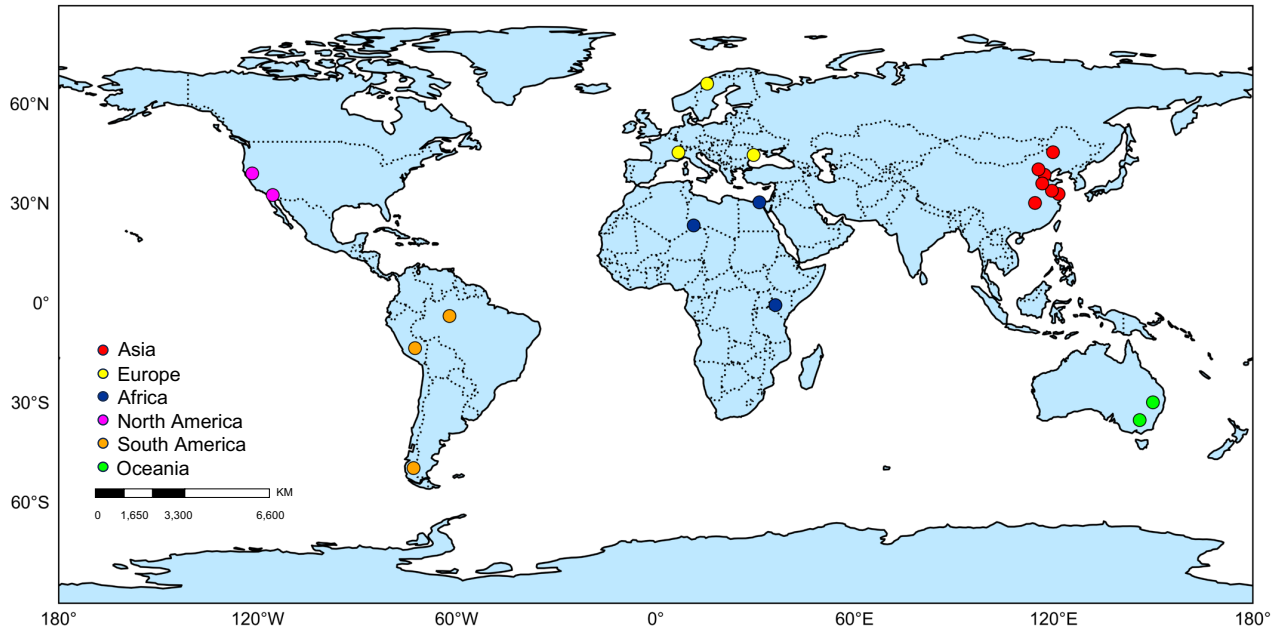


Figure 7: Global distribution and data samples of spatiotemporal fusion datasets.

Table 3
Common Spatiotemporal Fusion Datasets.

Dataset	Source	Resolution	Region	Link
CIA [43]	Landsat, MODIS	30m, 500m, 16 days	Coleambally, AU	Link
LGC [47]	Landsat-5 TM, MODIS	30m, 500m, 16 days	Lower Gwydir, AU	Link
MOD09GA [48]	MODIS	500m, Monthly	North China Plain	Link
BC [49]	Sentinel-2 MSI, S3 OLCI	10m, 300m, Monthly	SW Butte County, CA	Link
IC [49]	Sentinel-2 MSI, S3 OLCI	10m, 300m, Monthly	Imperial County, CA	Link
OISST [50]	AVHRR, Buoy, Ship	0.25° × 0.25°, Daily	Global Ocean	Link
OSTIA [50]	Multi-sat IR, MW, Buoy	0.05° × 0.05°, Daily	Global Ocean	Link
G1SST [50]	Geo, Polar Sats	0.01° × 0.01°, Daily	Global Ocean	Link
EARS [50]	ECMWF Model	0.25° × 0.25°, Hourly	Global Ocean	Link
In-situ [50]	Buoy Measurements	16 Stations, Hourly	Korean waters	Link
TRMM [51]	NASA GSFC PPS	0.25°, 3-hourly	50°N–50°S	Link
GridSat [51]	NOAA	0.07°, 3-hourly	70°S–70°N	Link
DEM [51]	USGS, NASA SRTM	90m, N/A	60°N–56°S	Link
Rain [51]	CMDC (China)	Point, 12-hourly	China	Link
S2 [52]	Sentinel-2	10m, 5-day revisit	Dafeng, China	Link
GOCI-II [52]	GOCI-II Satellite	500m, hourly	Dafeng, China	Link
Wuhan [53]	GF, Landsat	8m, 30m	Wuhan, China	Link
Daxing [12]	LS8 OLI, MODIS	30m, 500m, 8 days	Daxing, Beijing	Link
AHB [12]	LS8 OLI, MOD09GA	30m, 500m, 16 days	Ar Horqin Banner	Link
Tianjin [12]	LS8 OLI, MOD02HKM	30m, 500m, 16 days	Tianjin, China	Link
Terra [54]	Multi-source	0.1°, 3-hourly	Global	Link

Neural Networks (CNNs) [57], Transformer [58], Generative models [53], Sequence models [59], and other innovative architectures (such as graph neural networks [60], dual-branch fusion networks [61], multi-layer perceptrons [62], *etc.*). These models exhibit distinct features in terms of spatiotemporal modeling capabilities, performance optimization, and applicable scenarios, driving technological innovation in the remote sensing field [12, 26].

As shown in Figure 8, a summary of representative methods in remote sensing spatiotemporal fusion and their development over time is provided. Different colored timelines indicate representative models and corresponding years for CNN, GAN (Generative Adversarial Network), Diffusion, Transformer, sequence models, and other architectures [9, 32]. From 2017 to 2025, the application of various network architectures in this field has shown trends of diversification and refinement [9]. Meanwhile, Table 4 systematically summarizes the specific characteristics, loss functions, and performance metrics of different models, providing important references for in-depth analysis of the advantages, disadvantages, and usability of these methods.

2.3.1. Convolutional Neural Networks

Convolutional Neural Networks (CNNs) [84] have become the core architecture in spatiotemporal fusion research

in remote sensing since their breakthrough in computer vision [85]. The fundamental operation in CNNs is convolution, which can be mathematically expressed as:

$$y(i, j) = \sum_{m=0}^{M-1} \sum_{n=0}^{N-1} x(i+m, j+n) \cdot w(m, n), \quad (1)$$

where x represents the input image or feature map, w is the convolution kernel, y is the output feature map, i and j are the spatial coordinates in the output feature map, m and n are the indices for the kernel elements, and M and N represent the height and width of the convolution kernel, respectively. This operation enables CNNs to effectively capture spatial features at various levels of abstraction. Following convolution layers, pooling operations reduce spatial dimensions while preserving essential information:

$$y(i, j) = \max_{0 \leq m < s, 0 \leq n < s} x(i \cdot s + m, j \cdot s + n), \quad (2)$$

where s denotes the pooling window size, $y(i, j)$ is the output feature at position (i, j) , $x(i \cdot s + m, j \cdot s + n)$ represents the input feature at the corresponding position, and m and n are indices within the pooling window. Initially, CNNs demonstrated excellent performance in image classification

Table 4
A taxonomy of deep learning models for spatiotemporal fusion.

Network	Model	Year	Dataset	Loss Function	Metrics	Code
CNN	STFDCNN [45]	2018	CIA, LGC	MSE Loss	RMSE, ERGAS SAM, SSIM	N/A
	STFNet [63]	2019	Landsat, MODIS	MSE Loss, TC Loss	RMSE, CC SSIM	N/A
	EDCSTFN [64]	2019	MODIS, Landsat	Content Loss, Feature Loss, Vision Loss	RMSE, ERGAS SAM, SSIM	Link
	STF3DCNN [65]	2020	CIA, LGC, RDT	MSE Loss	CC, SAM PSNR, UIQI	N/A
	STTFN [66]	2021	Landsat, MODIS	Huber Loss	RMSE, SSIM	N/A
	MCDNet [67]	2021	CIA, LGC	Feature Loss, Content Loss	SSIM, RMSE CC, R^2	N/A
	MOST [68]	2021	Landsat-8, MODIS	L1 Loss	RMSE, SSIM SAM, ERGAS	N/A
	MUSTFN [69]	2022	Landsat-7, GaoFen-1	MAW-MSE Loss, VI Loss, SSIM Loss	RMSE, MAE rMAE	Link
	DenseSTF [44]	2022	CIA, LGC	MSE Loss	CC, RMSE SSIM	Link
	STF-EGFA [70]	2022	AHB, Daxing, Tianjin	Content Loss, Feature Loss, Visual Loss	SAM, PSNR CC, SSIM	N/A
	HCNNet [71]	2022	CIA, LGC, Daxing	MAE Loss, MS-SSIM Loss	RMSE, SAM ERGAS, CC	N/A
	MACNN [72]	2022	Landsat, MODIS	TC Loss, TD Loss	RMSE, SSIM CC, AD	N/A
	ECPW-STFN [43]	2024	CIA, Daxing	Wavelet Loss, Feature Loss, Vision Loss	RMSE, SSIM CC, SAM	Link
	MLKNet [73]	2024	CIA, DX, SW	Content loss, Feature loss, Visual loss	PSNR, SSIM SAM, CC	N/A
	RCAN-FSDAF [74]	2024	Landsat 8 OLI, MODIS13Q1	L1 Loss	RMSE, R, AD	N/A
CTSTFM [27]	2024	CIA, DX	L1 Loss	MAE, SAM, PSNR, SSIM	N/A	
Transformer	SwinSTFM [75]	2022	CIA, LGC, AHB	Charbonnier Loss, MS-SSIM Loss	RMSE, SSIM, SAM, ERGAS	Link
	TTSFNet [37]	2024	SST, SSS, SSHA, SSWA, SSTA	MSE Loss	R^2 , RMSE NRMSE	N/A
	STINet [35]	2024	Landsat-8, Sentinel-2	RMSE Loss	RMSE	N/A
	STFTN [58]	2024	CMIP6, SODA, GODAS, NMME	Weighted RMSE	RMSE, PCC	N/A
	MGSFormer [56]	2025	Beijingsites, Chinacities	MSE Loss	MSE, MAE, CORR	Link
GAN	MLFF-GAN [76]	2022	CIA, LGC	GAN Loss, L1 Loss, Spectrum Loss	MAE, RMSE, SSIM	Link
	GAN-STFM [4]	2022	CIA, LGC	LSGAN Loss, Feature Loss, Vision Loss	RMSE, SSIM	Link
	SS-STFM [36]	2024	LGC, BJGF6	GAN Loss	RMSE, AD	N/A
	HPLTS-GAN [46]	2024	CIA, LGC	LSGAN Loss, L1 Loss, Vision Loss	RMSE, SSIM	N/A
	DCDGAN-STF [53]	2024	CIA, LGC, Wuhan	GAN Loss, Visual Loss, Spectral Loss	SSIM, RMSE	Link
Diffusion	MFDGCN [77]	2022	PeMS_BAY	MAE Loss	MAE, RMSE, MAPE	N/A
	STFDiff [34]	2024	CIA, LGC	Simple Loss	RMSE, SSIM, ERGAS	Link

(continued on next page)

Table 4
Table 4 (continued).

Network	Model	Year	Dataset	Loss Function	Metrics	Code
Diffusion	DiffSTF [47]	2024	CIA, LGC	MSE Loss, Spectral Loss	RMSE, SAM, RASE, SSIM	N/A
	DiffSTSF [78]	2024	Gaofen-1 (PAN, MS, WFV)	MSE Loss, KL Divergenc	RMSE, SSIM, ERGAS	Link
Sequence Models	CNN-LSTM [51]	2020	TRMM, GridSat-B1, DEM, Rain Gauges	MSE Loss	RMSE, MAE, CC	N/A
	ConvLSTM [79]	2024	ERA5-land, GPM	N/A	FCA, TCA, OCA, R	N/A
	Geo-BiLSTMA [41]	2024	Xi'an	L2 Loss	RMSE, R^2	N/A
Others	STHGCN [80]	2022	METR-LA, PEMS-BAY, Solar Energy	Huber Loss, KL Divergence	MSE, RMSE	N/A
	MSFusion [81]	2022	CIA, LGC, DX	L1 Loss	SSIM, RMSE, ERGAS, SAM	N/A
	STFMLP [62]	2023	CIA, LGC	MSE Loss	RMSE, SAM	Link
	DSTFNet [82]	2023	GF-2, Sentinel-2	Tanimoto Loss	MCC, F1-score	N/A
	SDCS [83]	2024	CIA, LGC, AHB, Tianjin	L1 Loss, L2 Loss, SSIM Loss	RMSE, SSIM, SAM	Link

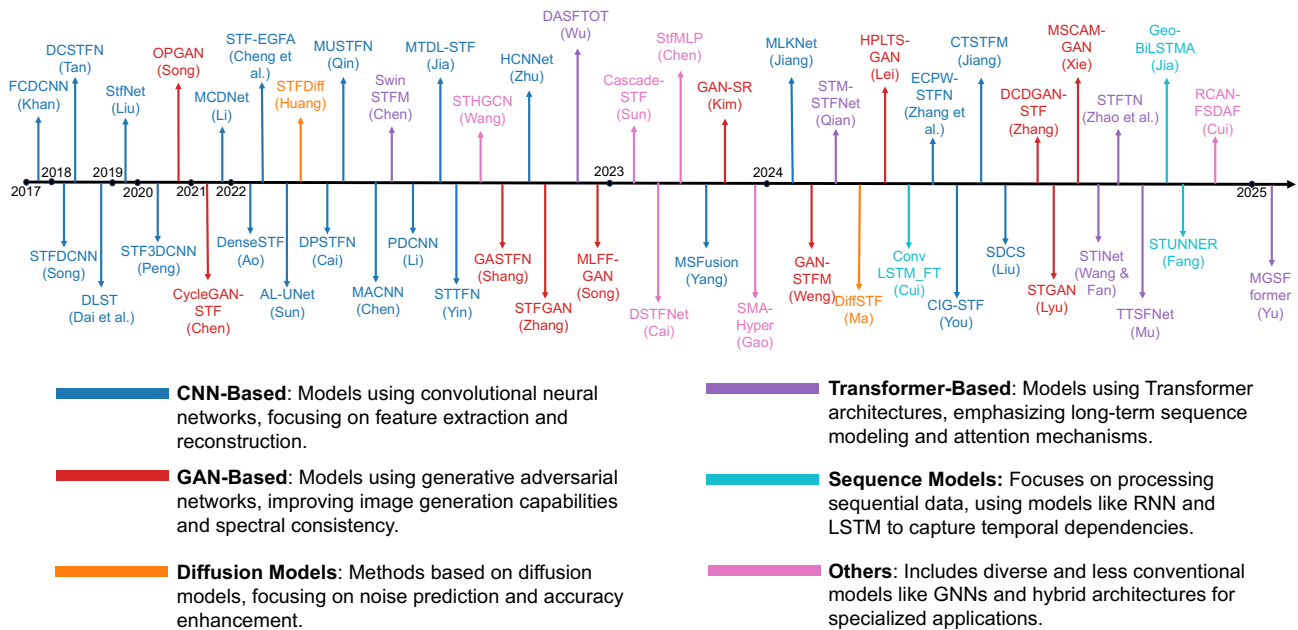


Figure 8: Timeline of deep learning-based spatiotemporal fusion methods and their classifications.

and recognition tasks with multi-layer convolution and pooling operations [86]. For example, AlexNet [28] significantly improved classification accuracy in the ImageNet competition with its deep convolutional structure. Later, VGGNet [87] deepened the network layers further, enhancing feature extraction capability. These successes prompted researchers to apply CNNs to remote sensing image processing to leverage their powerful spatial feature extraction ability for complex tasks such as land cover classification and change detection [88].

In early applications in remote sensing, STFD CNN [45] achieved spatiotemporal fusion of MODIS and Landsat images using nonlinear mapping and super-resolution convolutional networks, significantly improving fusion accuracy and efficiency. However, this model faced issues with insufficient detail retention and poor spectral consistency when handling complex terrains and rapidly changing land cover [89]. To address the inherent time-space conflict in spatiotemporal fusion, X. Liu *et al.* proposed STFNet [63], which uses a dual-stream CNN structure to process spatial and temporal features separately, combining temporal dependence and consistency through adaptive feature fusion. This architecture

mitigates the resolution trade-off between HSLT and HTLS data by explicitly modeling temporal dynamics in one stream while preserving spatial details in another. Specifically, STFNet [63] reconstructs the target fine image F_2 through an adaptive weighting strategy:

$$F_2 = \alpha * (F_1 + F_{12}) + (1 - \alpha) * (F_3 - F_{23}), \quad (3)$$

where F_{12} and F_{23} are fine difference images predicted from corresponding coarse ones and neighboring fine images, and α is a weighting parameter determined by the temporal similarity between coarse images. This adaptive fusion mechanism enables STFNet [63] to effectively balance the contribution of temporal information from both before and after the prediction time, thereby improving the reconstruction quality in areas with complex terrain and rapid land cover changes.

CNNs extract features through a hierarchical process, where lower-level spatial details evolve into more abstract semantic concepts across successive network layers. This progressive abstraction enables the network to capture increasingly complex patterns. The fundamental convolution operation shows how local receptive fields interact with kernels to produce feature maps that become inputs to deeper layers. This feature extraction mechanism has made CNNs particularly effective for spatiotemporal fusion tasks, where both spatial details and temporal changes must be accurately represented. Building on this fundamental architecture, Tan *et al.* proposed EDCSTFN [90], which optimized CNN application in spatiotemporal fusion through an improved composite loss function and enhanced data strategies. To enhance prediction image sharpness, EDCSTFN [90] replaced the traditional l_2 loss with a customized compound loss function that considers both prediction accuracy and image quality.

By combining convolution and deconvolution layers to extract both low and high frequency features, and integrating attention mechanisms (such as CBAM) [91], EDCSTFN [90] effectively addressed the spatiotemporal fidelity dilemma through frequency-aware feature separation and attention-guided fusion.

Further advancing this approach, Cai *et al.* introduced DPSTFN [92], which adopted a progressive fusion framework that combined pan-sharpening, super-resolution, and spatiotemporal fusion modules. Leveraging Residual Dense Blocks (RRDB) [93] and a decoupled spatial-spectral attention mechanism, DPSTFN [92] achieved enhanced fusion results by sequentially resolving spatial and temporal discrepancies. This hierarchical approach alleviates the time-space conflict through stage-wise refinement, where initial stages focus on spatial enhancement while subsequent layers handle temporal coherence.

Recent studies, such as CIG-STF [94] proposed by You *et al.*, explicitly use land cover change detection in spatiotemporal fusion to enhance model performance. CIG-STF [94] introduced a Change Information-Guided Enhancement Module to enhance the generation of superior final prediction results.

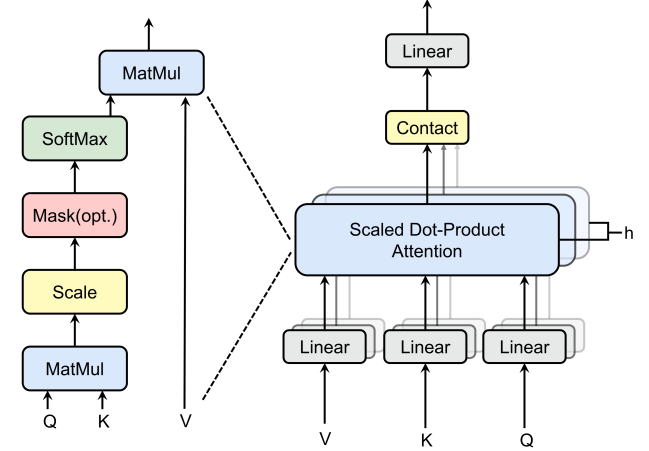


Figure 9: Multi-head attention mechanism in Transformer.

CIG-STF [94] designed a multi-scale dilated convolution feature extractor and a spatiotemporal fusion-change detection module, excelling in the reconstruction of sudden change areas and significantly enhancing the model's robustness in complex environments [95]. By incorporating change-aware temporal modeling, this framework dynamically adjusts spatial reconstruction intensity based on temporal change magnitude, thereby balancing the resolution conflict through adaptive feature weighting.

By gradually introducing multi-scale feature extraction, attention mechanisms, and change detection modules, CNNs continue to deepen their application in remote sensing spatiotemporal fusion, overcoming the limitations of earlier models and demonstrating higher fusion accuracy and adaptability [96, 97]. These continuous developments suggest that CNNs will continue to play an important role in future remote sensing spatiotemporal fusion research, driving further technological advancements and widespread applications [98, 99].

2.3.2. Transformer

Vaswani *et al.* [31] introduced the Transformer model to address sequence-to-sequence tasks like machine translation, text summarization, and speech recognition [100]. Unlike traditional recurrent neural networks, Transformer possesses a unique self-attention mechanism that effectively captures long-term dependencies while enabling more efficient parallel computing [101, 102]. Figure 9 illustrates Transformer's multi-head attention mechanism, including the matrix multiplication (MatMul) of query (Q), key (K), and value (V) matrices, scaling, optional masking, and SoftMax operations. The linear transformations of Q, K, and V in the scaled dot-product attention module converge to generate output representations (h). The self-attention mechanism can be formulated as:

$$\text{Attention}(Q, K, V) = \text{softmax}\left(\frac{QK^T}{\sqrt{d_k}}\right)V, \quad (4)$$

Within this foundational formula, the variables Q , K , and V correspond to query, key, and value matrices extracted from the input sequence, while d_k indicates the dimensionality of the key vectors. This distinctive network architecture has achieved exceptional results in natural language processing and has been widely applied across various domains, including CV, marking the beginning of Transformer applications in multimodal tasks [103, 104, 105].

Vision Transformer (ViT) [106] represents the beginning of Transformer applications in computer vision by dividing images into fixed-size patches and processing the flattened sequence of patches using Transformer. This sequence conversion can be represented as:

$$\mathbf{z}_0 = [\mathbf{x}_{\text{class}}; \mathbf{x}_p^1 \mathbf{E}; \mathbf{x}_p^2 \mathbf{E}; \dots; \mathbf{x}_p^N \mathbf{E}] + \mathbf{E}_{\text{pos}}. \quad (5)$$

Breaking down the components of this equation: the matrices $\mathbf{E} \in \mathbb{R}^{(P^2 \cdot C) \times D}$ and $\mathbf{E}_{\text{pos}} \in \mathbb{R}^{(N+1) \times D}$ establish the dimensional context, $\mathbf{x}_{\text{class}}$ represents a specialized learnable embedding comparable to BERT's [class] token, \mathbf{x}_p^n identifies the n -th image patch in the sequence, \mathbf{E} operates as the projection matrix for patch embeddings, while \mathbf{E}_{pos} contributes essential positional encoding. This approach has even surpassed traditional convolutional neural networks in multiple image classification benchmarks [107, 108]. However, ViT [106] has relative limitations, such as consuming excessive resources when processing high-resolution images [109, 110]. Subsequent researchers introduced hierarchical structures and sliding window self-attention mechanisms, effectively reducing computational complexity while maintaining excellent performance, enhancing Transformer's practicality in CV tasks and laying the foundation for its expansion into more complex applications [111, 112].

Remote sensing images typically possess high dimensionality and complex spatial features, presenting challenges in computational resources and modeling capabilities when processing large-scale remote sensing data [113, 114, 115]. To address these challenges, researchers began introducing Transformer's self-attention mechanism into remote sensing image processing to better capture spatial and spectral features [116]. Classic Transformer models like Swin Transformer [75] have been widely applied to remote sensing image classification, object detection, and other tasks [117]. As technology evolved, more innovative Transformer models emerged, driving applications in spatiotemporal fusion and other tasks, improving fusion accuracy while providing greater adaptability and robustness in computational complexity and detail preservation [118, 119].

STFormer [120] represents one model applying Transformer architecture to spatiotemporal fusion. To resolve the inherent conflict between temporal and spatial dimensions, STFormer [120] introduced a spatiotemporal self-attention mechanism capturing both temporal and spatial dependencies. This network architecture addresses the shortcomings of traditional methods that sacrifice spatial details while integrating temporal information. Nevertheless, STFormer [120] is limited by higher computational complexity when processing large-scale data, showing suboptimal performance in

practical applications. To effectively balance spatiotemporal conflicts and address computational limitations, Chen *et al.* proposed the Temporal-Swin Transformer [121], which maintains a delicate balance between spatial details and temporal dynamics through hierarchical processing of spatiotemporal self-attention mechanisms. This hierarchical approach significantly reduces computational complexity while preserving the model's ability to effectively capture both dimensions [122].

Subsequently, models like CFFormer [55] further improved the handling of spatiotemporal conflicts by combining GAN and Transformer architectures. Accurate modeling of temporal dynamics while maintaining high spatial resolution requires complementary advantages, leading researchers to introduce generative modules specifically designed to enhance spatial detail preservation. Through multi-scale feature fusion, these models improved adaptability to temporal changes in complex environments and heterogeneous data, thus balancing temporal and spatial information processing. MGSFormer [56] represents the latest approach to resolving spatiotemporal conflicts, not viewing spatial and temporal dimensions as opposing elements but introducing an integrated framework containing residual redundancy removal modules, spatiotemporal attention modules, and dynamic fusion modules. This framework simulates interactions between spatial and temporal features at multiple granularity levels, establishing a more harmonious relationship between these traditionally conflicting dimensions. MGSFormer [56] has demonstrated outstanding performance in fusion experiments across multiple datasets, better addressing the spatiotemporal conflict problem that has long plagued spatiotemporal fusion tasks.

2.3.3. Generative Models

Generative models work by learning the underlying distribution of input data to create new data samples [123, 124]. Their main goal is to simulate real-world data distributions and generate new data with similar statistical properties [125]. With the rapid development of deep learning, generative models have evolved from traditional probabilistic graphical models to deep generative networks [126]. In their early stages, generative models relied on traditional methods like Hidden Markov Models (HMM) [127] and Gaussian Mixture Models (GMM) [128], capturing data distributions and structures to generate new samples [129]. These approaches were primarily used for simpler data generation tasks because they were limited by data dimensionality and complexity [130].

The emergence of deep learning enabled further advancement of generative models [131]. Deep generative networks leverage neural networks to model complex data distributions, evolving into more powerful and flexible data generation methods. Typical examples include GANs and Variational Autoencoders (VAEs). Introduced by Goodfellow [29], GANs revolutionized generative modeling through adversarial training between a generator and a discriminator [132]. Their strength lies in generating highly realistic and diverse samples, greatly satisfying requirements for tasks

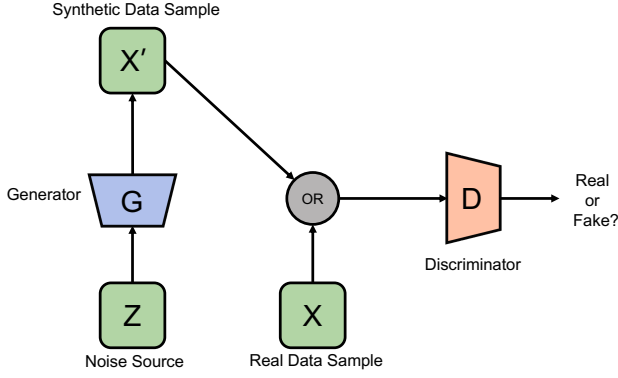


Figure 10: Basic GAN framework with generator (G) and discriminator (D).

such as image generation, image restoration, and style transfer. VAEs [133], on the other hand, learn latent distributions of data by maximizing the variational lower bound, proving highly effective in unsupervised learning and generative tasks. Although VAEs [133] have more stable training processes than GANs, the quality and diversity of their generated samples are typically lower [134, 135].

Diffusion models have brought new prospects to generative modeling in recent years. By simulating gradual “noising” of data and reverse denoising, these models can generate high-quality images while improving generation efficiency. These new models address some challenges faced by traditional generative models in detail recovery and training stability, demonstrating exceptional performance in areas such as image generation, image restoration, and super-resolution tasks [136, 137]. The continuous advancement of generative models has provided new solutions for data augmentation, image reconstruction, and fine-grained feature recovery, driving technological development in fields like CV, RS, and medical imaging.

Generative Adversarial Networks. GANs were first introduced by Goodfellow *et al.* [29], achieving high-quality data generation through adversarial training between a generator and a discriminator. As shown in Figure 10, the GAN framework consists of two competing neural networks: a generator (G) that transforms random noise \mathbf{z} from a noise source into synthetic data samples \mathbf{x}' , and a discriminator (D) that attempts to distinguish between real data samples \mathbf{x} and generated samples. The inputs are alternately fed to the discriminator through an OR gate, which then outputs a probability verdict of “Real or Fake?” for the incoming sample. Through this adversarial process, the generator progressively improves its ability to create realistic samples that can fool the discriminator. The core of this approach is formalized as a two-player minimax game, with the following value function $V(G, D)$:

$$\min_G \max_D V(D, G) = \mathbb{E}_{\mathbf{x} \sim p_{\text{data}}(\mathbf{x})} [\log D(\mathbf{x})] + \mathbb{E}_{\mathbf{z} \sim p_z(\mathbf{z})} [\log(1 - D(G(\mathbf{z})))] \quad (6)$$

Within this framework, the generator G transforms random noise \mathbf{z} into synthetic data through the mapping $G(\mathbf{z}; \theta_g)$, with θ_g comprising the generator’s learnable parameters. Conversely, the discriminator D calculates the likelihood that an input originated from actual data rather than being artificially generated. These expectations \mathbb{E} are calculated across the distribution of authentic data $p_{\text{data}}(\mathbf{x})$ and the distribution of noise inputs $p_z(\mathbf{z})$.

Undeniably, the GAN architecture pioneered a new era in generative models, though it often faces instability and mode collapse issues during training.

To address these limitations, Radford *et al.* proposed DCGAN [138], which introduced a fully convolutional network structure that made generators and discriminators more suitable for image data, improving the quality and stability of generated images. Subsequently, Arjovsky *et al.* introduced WGAN [30], effectively alleviating gradient vanishing problems by incorporating the Earth Mover’s distance, further enhancing GAN training stability and generative performance. In StyleGAN [139], Karras *et al.* achieved more refined control over generated images by separating content and style information, significantly improving the diversity and quality of generated images. The researchers developed a novel architectural approach where stylistic elements are controlled through weight modulation in the convolutional layers:

$$w'_{ijk} = s_i \cdot w_{ijk} \quad (7)$$

This equation illustrates how the original weights w_{ijk} are transformed into modulated weights w'_{ijk} by applying the style-specific scaling factor s_i to the i th input channel. The subscripts j and k identify the respective output channel and spatial position within the convolution operation. Following this modulation process, the resulting activations exhibit a standard deviation characterized by:

$$\sigma_j = \sqrt{\sum_{i,k} (w'_{ijk})^2} \quad (8)$$

To ensure computational stability and appropriate normalization, an additional scaling transformation is implemented:

$$w''_{ijk} = w'_{ijk} / \sqrt{\sum_{i,k} (w'_{ijk})^2 + \epsilon} \quad (9)$$

where the symbol w''_{ijk} denotes the weights after complete normalization, while ϵ represents a small positive constant that prevents division by zero. Through this sophisticated adaptive normalization system, the network achieves fine-grained stylistic control while maintaining robust and consistent training behavior.

These improvements laid the foundation for GAN applications in CV, establishing them as excellent techniques for high-quality image generation [140, 141]. Initially, GANs were primarily used for image generation tasks such as image synthesis and style transfer. GANs can meet the demands of

image restoration, enhancement, and synthesis by training generators to produce images similar to real data [142]. The emergence of StyleGAN [139] marked a major breakthrough in separating content and style in images, advancing fields like image editing and facial synthesis [143]. Additionally, GANs are widely applied to object detection and image classification tasks, where researchers combine generative networks with discriminators to enhance image feature learning, further improving model performance across various CV tasks [144].

In remote sensing spatiotemporal fusion, GANs play a unique role. GAN models are particularly suitable for resolving the fundamental conflict between temporal and spatial dimensions, as high spatial resolution typically comes with lower temporal frequency, while high temporal resolution usually sacrifices spatial details. For example, Song *et al.*'s MLFF-GAN [76] effectively addresses spatiotemporal conflicts using a U-net encoding-decoding structure, Adaptive Instance Normalization (AdaIN) [145], and Attention Modules (AM) [146]. This architecture processes spatial and temporal information simultaneously, enabling the model to effectively balance spatial resolution and temporal dynamics when facing issues such as spatiotemporal resolution differences, dramatic land cover changes, and sensor system errors.

To solve spatial coherence problems that often occur when fusing images from different time points, Weng *et al.*'s GAN-STFM [36] offers a novel solution. Their seamless splicing mechanism specifically addresses the splicing gap issues common in traditional spatiotemporal fusion methods, significantly improving the visual quality and spectral consistency of generated images, demonstrating GAN's excellent performance in helping bridge spatial integrity and temporal dynamics.

Lei *et al.* [46] further refined the handling of spatiotemporal conflicts by introducing an Adaptive Spatial Distribution Transformation (ASDT) [147]. In heterogeneous regions where balancing spatial details and temporal changes is particularly challenging, their model significantly improves spatiotemporal consistency by adaptively adjusting spatial distribution based on temporal context. This allows the model to maintain high spatial fidelity while effectively tracking temporal evolution, directly addressing the core contradiction in spatiotemporal fusion applications.

Zhang *et al.*'s DCDGAN-STF [53] addresses spatiotemporal conflicts by introducing multi-scale deformable convolution distillation mechanisms and teacher-student correlation distillation mechanisms. Their deformable convolution mechanism captures spatiotemporal differences between multi-temporal images, enabling the model to flexibly extract features of irregularly shaped changes. Additionally, their knowledge distillation innovation uses KL divergence to measure feature similarity between teacher and student networks, significantly improving texture detail recovery while maintaining temporal prediction accuracy, demonstrating its balanced capability in processing spatiotemporal information. **Diffusion Models.** Diffusion models were actually developed inspired by diffusion processes in statistical physics, representing a breakthrough advancement in the field of generative

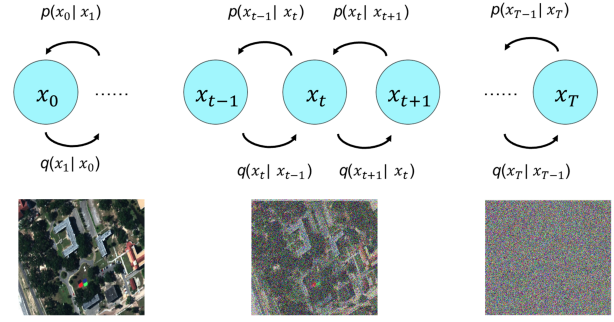


Figure 11: Forward and reverse process in diffusion models.

modeling in recent years. As shown in Figure 11, diffusion models operate via two key processes: a forward process (denoted by $q(x_t | x_{t-1})$) that progressively adds noise to data samples, and a reverse process (denoted by $p(x_{t-1} | x_t)$) that learns to denoise and recover the original data. The figure shows the Markov chain from the clean image x_0 through intermediate noisy states (x_{t-1}, x_t, x_{t+1}) to the fully noisy state x_T . The bottom images demonstrate this process visually on a remote sensing example, where the left image shows the original clean data, the middle image shows a partially noised state, and the right image shows the completely noisy state resembling pure Gaussian noise. During training, the model learns to reverse this noise addition process to generate new data samples.

Watson *et al.* used Denoising Diffusion Probabilistic Models (DDPM) [148], which established a forward diffusion process that systematically adds Gaussian noise to data through a Markov chain:

$$q(x_t | x_{t-1}) = \mathcal{N}(x_t; \sqrt{1 - \beta_t} x_{t-1}, \beta_t \mathbf{I}). \quad (10)$$

Within this elegant framework, $q(x_t | x_{t-1})$ expresses the probability distribution of x_t conditional on x_{t-1} , while x_t indicates the noise-corrupted sample at time point t . The coefficient $\beta_t \in (0, 1)$ serves as the noise intensity scheduler, and \mathbf{I} represents the identity matrix. Here, $\mathcal{N}(\mu, \sigma^2)$ signifies a normal distribution characterized by mean μ and variance σ^2 . DDPM [148] subsequently optimizes a neural architecture ϵ_θ to reconstruct the reverse denoising trajectory by minimizing:

$$\mathcal{L} = \mathbb{E}_{t, x_0, \epsilon} [||\epsilon - \epsilon_\theta(x_t, t)||^2]. \quad (11)$$

In this optimization objective, \mathcal{L} corresponds to the error metric, \mathbb{E} signifies expectation, and ϵ_θ denotes the neural predictor with trainable parameters θ designed to estimate noise components. The term $\epsilon \sim \mathcal{N}(0, \mathbf{I})$ refers to the random noise initially injected into the clean data x_0 , while t indicates the temporal position in the diffusion sequence, and $|| \cdot ||^2$ quantifies the squared Euclidean distance. This innovative approach has allowed diffusion-based architectures to surpass GANs in generation quality while avoiding their notorious training instabilities.

Although DDPM's [148] generation quality is impressive, it requires multiple sampling steps, resulting in slower generation speed, which limits its use in practical applications. To address this issue, Song *et al.* proposed Denoising Diffusion Implicit Models (DDIM) [148], which accelerated the sampling process through a non-Markovian diffusion process:

$$x_{t-1} = \sqrt{\alpha_{t-1}} \left(\frac{x_t - \sqrt{1 - \alpha_t} \epsilon_\theta(x_t, t)}{\sqrt{\alpha_t}} \right) + \sqrt{1 - \alpha_{t-1} - \sigma_t^2} \cdot \epsilon_\theta(x_t, t) + \sigma_t \epsilon, \quad (12)$$

where x_{t-1} represents the reconstructed sample at step $t - 1$, x_t denotes the current noisy input, and $\alpha_t = \prod_{i=1}^t (1 - \beta_i)$ captures the cumulative effect of the noise schedule across timesteps. The function $\epsilon_\theta(x_t, t)$ embodies the neural network's prediction of noise components, while σ_t functions as a control parameter governing the sampling process's stochastic properties, and $\epsilon \sim \mathcal{N}(0, \mathbf{I})$ introduces fresh Gaussian noise to maintain generation diversity, dramatically enhancing computational efficiency without sacrificing output quality.

Rombach *et al.* introduced latent diffusion models [149], further advancing the field by operating in a compressed latent space, greatly reducing computational complexity and making diffusion models more efficient in high-resolution image generation tasks.

In CV, the superior performance of diffusion models has gradually emerged [150, 151]. In tasks such as image restoration, style transfer, and super-resolution, diffusion models overcome some limitations of traditional generative models through their gradual denoising approach, generating clearer and more detailed images [152]. Subsequently, the efficiency and powerful detail recovery capabilities of diffusion models have also begun to be applied in other fields [153, 154].

In remote sensing spatiotemporal fusion research, diffusion models provide new methods for resolving the fundamental conflict between temporal and spatial dimensions through gradual denoising. Previous methods typically struggled to maintain both detailed spatial features and accurate temporal dynamics when fusing HSLT and HTLS data, while diffusion models offer a natural framework to reconcile this contradiction. Ma *et al.* proposed DiffSTF [47], designing a conditional diffusion model specifically for spatiotemporal fusion to address spatiotemporal conflicts. They recognized that the inherent gradual denoising process of diffusion models provides a natural framework for harmonizing temporal and spatial information. By combining an encoder-decoder structure with residual blocks and Transformer blocks, DiffSTF [47] effectively captures both global temporal patterns and local spatial features simultaneously, resolving the balance between spatial resolution and temporal dynamics more effectively than previous methods.

To further optimize the handling of spatiotemporal conflicts, Huang *et al.* proposed the STFDiff [34]. During the noise prediction process, the tension between spatial and temporal information becomes particularly evident. They

developed a dual-stream encoder specifically designed to process spatial and temporal information through independent but interconnected paths, allowing the model to maintain the features of each dimension while exchanging cross-dimensional information at key points in the processing pipeline. This approach combines innovative temporal embedding techniques that transform discrete time variables into continuous vector representations. By incorporating efficient noise prediction modules, STFDiff [34] achieves a more balanced fusion of spatial details and temporal dynamics, significantly improving the structural similarity index and spectral fidelity across multiple datasets.

Diffusion-based models optimize the efficiency and effectiveness of the fusion process by introducing multi-scale feature extraction and dynamic modules aimed at harmonizing spatial and temporal information. Unlike previous approaches that viewed spatiotemporal conflicts as limitations to be managed, these diffusion models consider this tension as a core part of their design, gradually harmonizing spatial and temporal features through an iterative denoising process. This undoubtedly demonstrates the powerful potential of diffusion models in resolving spatiotemporal conflicts in remote sensing spatiotemporal fusion.

2.3.4. Sequence Models

Sequence models can be used to efficiently simulate dynamic changes in time series through their recursive structure and memory mechanisms, making them widely used in spatiotemporal fusion research [155]. The development of sequence models mainly includes Recurrent Neural Networks (RNNs) [156] and their enhanced versions, which include Gated Recurrent Units (GRU) [157] and Long Short-Term Memory (LSTM) networks [158]. Such models, which are very effective in time series modeling, provide strong technical support for handling long-term dependencies and predicting dynamic changes.

Recurrent Neural Network. RNNs originated in the 1980s and are a form of neural network structure that recursively passes hidden layer states. The main advantage of RNNs lies in their capacity to capture time dependencies in input data. The typical RNN formulation can be written as:

$$h_t = \sigma(W_h h_{t-1} + W_x x_t + b). \quad (13)$$

In this concise formulation, h_t denotes the network's internal representation at temporal point t , while h_{t-1} captures the memory state from the previous step. The variable x_t encodes the current input information, and the transformation matrices W_h and W_x govern the influence of historical context and new data respectively. The vector b introduces learning flexibility, and σ represents the non-linear transformation function (commonly implemented as tanh or ReLU) that enables the network to capture complex patterns. Traditional RNNs, however, struggle with processing long time series information due to issues such as vanishing and exploding gradients [156].

With the effective application of RNNs in sectors such as natural language processing, scholars suggested many

improved models to increase their computing efficiency and memory capabilities [159, 160]. For instance, Bidirectional RNNs (such as Bidirectional LSTM) enhance the model’s understanding of sequence context by processing both forward and backward time dependencies. GRU [157] simplifies the gating structure, reducing model parameters and improving computational efficiency [161]. These improvements not only increase the model’s performance in sequence modeling activities but also set the basis for their use in CV tasks such as video analysis and action recognition [162].

In remote sensing, RNNs and their variants offer a distinctive approach to the conflict between temporal and spatial dimensions. Unlike other models that often struggle to balance high spatial resolution with accurate temporal dynamics, RNNs naturally prioritize the temporal aspect through their sequential processing architecture. This temporal focus provides an alternative perspective on the HSLT and HTLS tension inherent in remote sensing data. Models like STUNNER [163] address this time-space conflict by introducing a dual-stream structure combined with Time Difference Networks (TDN) [164] and Spatiotemporal Trajectory Networks (STTN) [165]. This architecture effectively reconciles temporal and spatial priorities by separating their processing pathways, allowing STUNNER to efficiently model non-stationary sequences and short-term instantaneous changes while preserving spatial context. In particular, the TDN [164] component employs a stacked TDiff-LSTM structure to model stationarity in time series through layer-by-layer feature differencing. This dual-stream approach creates a more balanced relationship between temporal evolution and spatial integrity, significantly outperforming mainstream models such as TrajGRU [166], PredRNN [167], and MetNet [163]. These advances in RNN architectures provide effective guidance for addressing the fundamental temporal-spatial conflict in remote sensing. By optimizing temporal information flow while preserving spatial context, these models enable the development of more accurate and robust fusion technologies that better balance the competing requirements of temporal dynamics and spatial detail preservation.

Long Short-Term Memory. Long Short-Term Memory (LSTM) networks have significantly surpassed traditional Recurrent Neural Networks (RNNs) in handling long-term dependencies, thereby enhancing the performance of sequence models [158]. Their advanced gating mechanisms enable efficient processing of extended sequences, overcoming the limitations of conventional RNNs [168]. Continuous refinements in architecture have expanded their applicability to more complex tasks. LSTM and its variants offer a sophisticated solution to the inherent temporal-spatial conflict in remote sensing spatiotemporal fusion. Their selective memory capabilities provide a distinct advantage in accurately capturing temporal evolution, which helps reconcile the challenge of maintaining high spatial resolution with temporal precision. These models excel at balancing competing demands in fusion tasks.

LSTM networks are mainly composed of three dedicated gate units: input gate, forget gate, and output gate, which control the flow of information in a selective manner. The architectural brilliance of LSTM networks emerges from their innovative triple-gate mechanism (input (i_t), forget (f_t), and output (o_t) gates), orchestrating precise information management. The mathematical machinery of LSTM with peephole connections unfolds through these relationships:

$$f_t = \sigma(W_{xf}x_t + W_{hf}H_{t-1} + W_{cf} \odot C_{t-1} + b_f), \quad (14)$$

$$C_t = f_t \odot C_{t-1} + i_t \odot \tanh(W_{xc}x_t + W_{hc}H_{t-1} + b_c), \quad (15)$$

where f_t embodies the forgetting mechanism determining which historical information should be retained or discarded, while i_t functions as the information gatekeeper controlling the flow of new data into the memory. The term C_t represents the updated memory reservoir that preserves long-term dependencies, building upon its previous state C_{t-1} . The activation function σ constrains outputs to the range (0,1), creating continuous gating behaviors, while \tanh normalizes values between -1 and 1. The notation \odot indicates element-wise multiplication, enabling selective information filtering. The parameters W_{xf} , W_{hf} , W_{cf} , W_{xc} , and W_{hc} constitute learnable transformation matrices for their respective pathways, with x_t representing the current input vector, H_{t-1} capturing previous output state, and b_f and b_c providing adjustable bias values. Particularly noteworthy is the peephole connection component ($W_{cf} \odot C_{t-1}$), which creates direct memory access pathways, substantially enhancing the network’s capacity to capture precise temporal dependencies.

This somewhat intricate gating mechanism proves ideal for spatiotemporal fusion tasks that require a careful balance between spatial and temporal resolutions. L-UNet [59] combines convolutional layers, which are responsible for extracting spatial features, with LSTM layers, merging complementary architectural strengths to achieve effective spatiotemporal modeling while maintaining a delicate equilibrium.

ConvLSTM [79] fuses the LSTM framework with convolutional operations. By preserving LSTM’s robust temporal memory and leveraging convolutions to capture spatial dependencies, it offers a unified solution for challenging applications such as soil freeze/thaw monitoring. As dataset sizes increase and environmental complexity intensifies, however, ConvLSTM [79] faces practical issues related to computational resources and model intricacy when managing highly dynamic spatiotemporal interactions.

Geo-BiLSTM [41] combines direct LSTM modules with an attention mechanism to fine-tune the balance between spatial and temporal priorities. Its attention process assigns adaptive weights to spatial features based on the relevance of different temporal orders, while a bidirectional design captures context from both earlier and later time steps. This composite approach cultivates a refined equilibrium between dimensions, thereby boosting the model’s capacity to manage intricate spatiotemporal relationships while preserving all essential details. This advantage proves significant for predicting remote sensing data.

2.3.5. Other Models

Beyond these mainstream models, various architectures have demonstrated unique advantages in remote sensing spatiotemporal fusion, including Graph Neural Networks (GNN) [169], Multilayer Perceptrons (MLP) [62], and Dual-branch Fusion Networks [61]. These alternative approaches complement the capabilities of sequence-based models, offering specialized solutions for particular spatiotemporal fusion challenges.

GNNs can model spatial topological relationships between data through graph structures, making them suitable for tasks involving regional interactions and spatiotemporal dependencies [60]. STHGCN [80] proposed by Wang *et al.* combines multiple graph convolution modules with dynamic higher-order temporal difference convolution modules, effectively extracting higher-order spatial and temporal dependencies and greatly improving traffic flow prediction accuracy. Gao *et al.*'s SMA-Hyper [170] addresses the limitations of STHGCN [80] in handling multi-view relationships and sparse data. SMA-Hyper [170] adopts an adaptive multi-view hypergraph architecture with attention mechanisms to dynamically model higher-order cross-regional dependencies, significantly improving prediction performance on sparse data and enhancing model generalization capability and prediction accuracy.

As lightweight neural network architectures, MLPs offer extremely high computational efficiency with fewer parameter requirements. The STFMLP [62] proposed by Chen *et al.* replaces traditional CNNs for feature extraction with multi-layer perceptrons, combining Feature Pyramid Networks (FPN) [171] and temporal difference constraints to effectively enhance multi-scale feature extraction and prediction performance. This approach significantly reduces computational complexity, overcoming the computational resource consumption problems of traditional CNNs when modeling complex spatiotemporal relationships, providing a solid foundation for MLP-based complex tasks [172, 173].

Dual-branch Fusion Networks achieve exceptional modeling accuracy in multi-source remote sensing data fusion by processing features from different dimensions (such as space and time) separately. The DSTFNet [82] proposed by Cai *et al.* combines very high resolution (VHR) [174] images with medium resolution (MRSITS) data [175], using independent spatial and temporal branches to extract dynamic texture and spectral features, while optimizing the feature fusion process through attention mechanisms. This dual-branch structure effectively integrates multi-source data, overcoming the limitations of single-branch models in feature extraction and fusion, greatly improving the accuracy of farmland boundary detection and zoning tasks, and demonstrating its generalization capability and robustness across different regions [61].

To better showcase the advantages, disadvantages, and potential improvements of various deep learning architectures in remote sensing spatiotemporal fusion tasks, Table 5 provides a comprehensive comparison.

2.4. Evaluation Metrics

Evaluation metrics measure the accuracy of model predictions and provide benchmarks for comparing different STF methods [74, 176, 177]. Table 6 lists some commonly used evaluation metrics in this field.

2.4.1. Root Mean Square Error

$$RMSE = \sqrt{\frac{1}{n} \sum_{i=1}^n (y_i - \hat{y}_i)^2}, \quad (16)$$

where y_i stands for the actual value, \hat{y}_i indicates the predicted value, and n signifies the total number of samples considered.

RMSE quantifies the difference between predicted and actual values, measuring the magnitude of prediction errors [70, 178]. Lower RMSE values indicate more accurate predictions, with values approaching zero signifying minimal differences between predicted and actual values [179, 180].

2.4.2. Peak Signal-to-Noise Ratio

$$PSNR = 10 \cdot \log_{10} \left(\frac{MAX_I^2}{MSE} \right), \quad (17)$$

where MAX_I denotes the maximum possible pixel value in the image, while MSE refers to the Mean Squared Error between the reconstructed and reference images.

PSNR represents the ratio between the maximum possible power of a signal and the power of corrupting noise affecting its representation quality [72, 75]. This metric is frequently employed to measure signal reconstruction quality in domains such as image compression [44, 71].

2.4.3. Mean Absolute Error

$$MAE = \frac{1}{n} \sum_{i=1}^n |y_i - \hat{y}_i|, \quad (18)$$

where $|y_i - \hat{y}_i|$ signifies the absolute difference between the actual value y_i and the predicted value \hat{y}_i for the i -th sample, while n represents the total number of samples.

MAE represents the average of absolute errors between predicted and observed values [181]. Unlike RMSE, MAE exhibits lower sensitivity to outliers, making it particularly suitable for datasets containing a limited number of extreme values [182, 183].

2.4.4. Structural Similarity Index

$$SSIM(x, y) = \frac{(2\mu_x\mu_y + C_1)(2\sigma_{xy} + C_2)}{(\mu_x^2 + \mu_y^2 + C_1)(\sigma_x^2 + \sigma_y^2 + C_2)}. \quad (19)$$

The parameters of this equation are as follows: μ_x and μ_y represent the mean intensities, σ_x^2 and σ_y^2 correspond to the

Table 5
Comparison of network architectures for remote sensing spatiotemporal fusion.

Network	Advantages	Disadvantages	Potential Improvements
CNN	Strong spatial feature extraction. Efficient parameter sharing. Well-established in remote sensing.	Limited for long-range dependencies. Poor with non-linear changes. High computational costs for high-resolution images.	Integrate attention mechanisms. Improve multi-scale feature fusion. Introduce deformable convolutions. Develop specialized loss functions.
Transformer	Excellent for long-range dependencies. Effective global context processing. Superior in multi-temporal data fusion.	Quadratic complexity with image size. High memory requirements. Requires more data than CNNs.	Develop hierarchical processing. Create hybrid CNN-Transformer models. Design efficient attention computation. Improve detail preservation.
GAN	High-quality image generation. Handles complex transformations. Strong adaptability to heterogeneous data.	Training instability issues. High computational demands. Often prioritizes visual over spectral quality.	Implement stable training strategies. Improve spectral fidelity. Combine with attention mechanisms. Develop distillation approaches.
Diffusion Models	Superior detail restoration. Stable training. High-quality outputs with better structure preservation.	Slow generation process. High computational demands. Limited real-time applicability. Complex parameter tuning.	Develop accelerated sampling. Design latent-space models. Combine with encoder-decoder structures. Research conditional models.
Sequence Models	Excellent time series modeling. Effective for temporal predictions. Strong in change detection with efficient training.	Inefficient with spatial data. Limited capacity for long sequences. Less effective with complex spatial structures.	Combine with convolutions. Introduce bidirectional structures. Integrate attention mechanisms. Develop multi-stream architectures.

Table 6
Common Evaluation Metrics for Remote Sensing Spatiotemporal Fusion.

Metric	Description	Advantages	Limitations
MSE	Average squared differences between predicted and actual values for regression tasks.	Simple calculation, penalizes large errors effectively.	Overly sensitive to outliers, unintuitive units.
RMSE	Square root of MSE, used in fusion quality assessment.	Same units as original data, intuitive interpretation.	Disproportionately emphasizes large errors.
NRMSE	RMSE normalized by data range for cross-dataset comparison.	Enables comparison across different scales and sensors.	Depends on maximum and minimum values.
PSNR	Logarithmic signal-to-noise ratio for image quality assessment.	Standard metric for image quality with established thresholds.	Poor correlation with human visual perception.
MAE	Average absolute differences, suitable for outlier-prone data.	More robust to outliers than RMSE, equal error weighting.	Gradient issues during optimization.
SSIM	Structural similarity based on luminance, contrast, and structure.	Aligned with human perception of image quality.	Computationally complex, less sensitive to certain degradations.
PCC	Linear correlation measurement for image similarity assessment.	Clear [-1,1] range, captures global correlation patterns.	Only detects linear relationships.
R^2	Proportion of variance explained in regression evaluation.	Direct interpretation of model fit quality.	Unstable with small samples, misleading when assumptions violated.
SAM	Spectral angle measurement for spectral analysis.	Preserves spectral signatures, invariant to illumination scaling.	Ignores magnitude differences between spectra.

variances, and σ_{xy} describes the covariance between images x and y . The constants C_1 and C_2 are incorporated to maintain numerical stability.

SSIM evaluates the similarity between two images and is commonly used to measure the similarity between images before and after distortion, as well as to assess the authenticity of model-generated images [4, 59, 81].

2.4.5. Spectral Angle Mapper

$$SAM = \arccos \left(\frac{\sum_{i=1}^n x_i y_i}{\sqrt{\sum_{i=1}^n x_i^2} \sqrt{\sum_{i=1}^n y_i^2}} \right). \quad (20)$$

For this metric, x_i and y_i represent the spectral vectors of the predicted and reference images, respectively, while n indicates the number of spectral bands considered in the analysis.

SAM is applicable for evaluating spectral consistency in multispectral and hyperspectral remote sensing applications [184, 185].

2.4.6. Relative Dimensionless Global Error in Synthesis

$$ERGAS = 100 \cdot \frac{h}{l} \sqrt{\frac{1}{N} \sum_{i=1}^N \left(\frac{RMSE_i}{\mu_i} \right)^2}. \quad (21)$$

The equation utilizes several variables: h and l denote the spatial resolution of high and low-resolution images respectively, N symbolizes the number of spectral bands, $RMSE_i$ represents the Root Mean Square Error for band i , and μ_i corresponds to the mean value of the i -th band in the reference image.

ERGAS is frequently used to assess remote sensing image quality, typically expressed as a percentage [186, 187]. Lower ERGAS values indicate higher image quality [57, 67]. This metric considers mean square error, root mean square error, and brightness information to provide a comprehensive assessment of image processing or compression algorithm performance [68, 188].

When comparing and optimizing model performance, researchers rely on evaluation metric systems [88, 90]. By selecting and combining these common evaluation metrics, researchers can comprehensively assess a model's spatiotemporal reconstruction capabilities from multiple perspectives, compare the advantages and disadvantages of different models, and support further optimization of spatiotemporal fusion algorithms [45, 75, 90].

2.5. Applications of Spatiotemporal Fusion

Spatiotemporal fusion combines images of varying spatial and temporal resolutions to predict high-resolution outputs, a capability that is critical for remote sensing data processing in urban planning, disaster assessment, ecological monitoring, and climate change research [6, 13].

2.5.1. Ecology Monitoring

In agricultural monitoring, Xiao *et al.* [9] describe how this technique integrates MODIS's low spatial but high temporal resolution data with Landsat's high spatial but low temporal resolution imagery, yielding outputs that capture both fine spatial detail and dynamic temporal changes. This integration proves invaluable for tracking crop growth and developmental stage transitions. Li *et al.* [12] further highlight its efficacy in capturing the dynamic evolution of agricultural land, particularly when monitoring crop cycles and land-use modifications. Focusing on broader ecosystem surveillance, shifts in forest cover and species distribution often command primary attention. Belgiu and Stein [6] assert that spatiotemporal fusion methods adeptly bridge data gaps caused by cloud cover, a benefit that is indispensable in tropical regions where such obstructions are frequent.

2.5.2. Urban Planning

Spatiotemporal fusion methods have also gained attention in urban monitoring and planning. Since satellite images in urban areas require high spatial and temporal resolution, spatiotemporal fusion can provide more precise data for urban expansion monitoring. By combining HTLS data with HSLT data, urban land use and expansion can be tracked more effectively, providing decision support for urban planning [174].

2.5.3. Disaster Monitoring and Assessment

Spatiotemporal fusion technology demonstrates exceptional value throughout the full cycle of natural disaster monitoring and assessment, particularly in the refined monitoring of sudden disasters such as floods, droughts, and forest fires [49]. Through intelligent coordination of heterogeneous spatiotemporal resolution data, this technology rapidly reconstructs high-precision impact assessment maps during the critical post-disaster period. In forest fire ecological recovery monitoring, Xiao and colleagues have verified that fused high-resolution remote sensing images can precisely track vegetation succession trajectories in burned areas [9]. Even more groundbreaking is the technology's ability to construct dynamic damage assessment heat maps based on coordinated observation systems, providing spatial decision support for flood emergency response at the minute level. This represents a revolutionary advancement that has significantly enhanced the efficiency of traditional damage assessment [48, 54].

2.5.4. Climate Change Research

Against the backdrop of accelerating global climate system evolution, spatiotemporal fusion technology has become a crucial key to decoding climate-environment feedback mechanisms [58]. Its distinctive advantage lies in reconstructing global environmental monitoring sequence data with both spatial and temporal precision, thereby providing multidimensional observational benchmarks for climate sensitivity analysis. Recent studies have shown that this technology not only captures the spatiotemporal heterogeneity of large-scale temperature and humidity fields but also constructs ecological response fingerprint maps. This ability to decouple

climate signals from environmental feedback provides a novel perspective for revealing the nonlinear interaction mechanisms between climate and ecosystems in the context of the geologic era dominated by contemporary human activities [50].

3. Challenges

This section examines various challenges encountered during the development and application of remote sensing spatiotemporal fusion technologies. Breaking through these limitations requires researchers to innovate existing technologies, develop deeper understanding of these problems, and provide solutions that support further advancement in spatiotemporal fusion applications.

3.1. Time-Space Conflict

In the realm of remote sensing image fusion, mismatched temporal and spatial resolutions between sensors lead to fundamental conflicts in data harmonization. Inconsistencies in temporal resolution can lead to deviations in the fusion results along the time dimension, particularly in areas experiencing rapid surface changes, such as vegetation growth and urban expansion. In such cases, the fusion outcomes may fail to accurately capture these dynamic changes. Similarly, discrepancies in spatial resolution can result in errors in the spatial dimension, which is especially critical for applications requiring high spatial precision, such as urban mapping and agricultural monitoring. Beyond the fundamental conflicts arising from mismatched temporal and spatial resolutions, several other issues contribute to the complexity of spatiotemporal fusion. These include mismatched temporal scales, asynchronous data acquisition, differences in sensor characteristics (*e.g.*, spectral bands, viewing geometry, radiometric calibration), incompatibilities in data processing methods (*e.g.*, radiometric correction, geometric correction, and atmospheric correction), and surface heterogeneity, *etc.* In essence, harmonizing time-space conflict requires a holistic approach that not only optimizes the trade-off between temporal and spatial resolutions but also accounts for the entire data lifecycle—from acquisition and preprocessing to fusion, validation, and ultimately the production of high-quality fusion products for application.

3.2. Generalization of Deep Models

While numerous studies report impressive performance metrics on specific datasets, very few systematically evaluate how these models perform when applied to entirely new datasets or satellite pairs without re-training or fine-tuning. Deep models possess inherent limitations, particularly in terms of poor generalizability. Models that perform exceptionally well within their training distribution often experience significant performance degradation when confronted with data from different geographical regions, seasons, or imaging conditions. The generalization challenge extends beyond spectral differences to include variations in spatial resolution ratios, temporal gaps, and regional landscape characteristics [136]. A model trained on agricultural landscapes may

fail to generalize to urban environments. Similarly, models optimized for specific seasonal transitions might perform poorly during other seasonal changes. These limitations highlight the need for more robust approaches that can maintain performance across diverse scenarios. Furthermore, current deep architectures for spatiotemporal fusion typically operate with fixed input band configurations. This architectural rigidity means they cannot process data with different channel inputs than those used during training. This further restricts the practical application capabilities of these models, leading to a complete loss of generalization ability.

3.3. Large Datasets at Scale

The advancement of deep learning in remote sensing spatiotemporal fusion is significantly constrained by the limited scale and diversity of available datasets. Unlike the computer vision field, which benefits from large-scale and diverse datasets like ImageNet [189] and COCO [190] that provide extensive coverage and rich annotations, remote sensing spatiotemporal fusion datasets often fall short. These datasets typically lack the volume and variety needed to effectively train deep learning models that can generalize well across different regions and conditions. For example, while ImageNet [189] contains millions of images across thousands of categories, supporting robust feature learning, remote sensing datasets such as Landsat and MODIS, though valuable, offer fewer samples and less diversity in terms of geographic coverage, environmental conditions, and sensor types. This limitation results in models that perform well on specific datasets but struggle when applied to new or varied scenarios. Additionally, the high cost and complexity of acquiring and processing remote sensing data further hinder the creation of larger and more diverse datasets. The absence of comprehensive benchmarks comparable to those in computer vision limits the ability of researchers to fully leverage the potential of deep learning, emphasizing the urgent need for more extensive and varied datasets to drive innovation in spatiotemporal fusion technology.

3.4. Multi-source Heterogeneous Fusion

The diversification of technologies and observation platforms has led to remote sensing data from different sources exhibiting significant heterogeneity across spatial resolution, spectral range, band configuration, and viewing angles [26, 191, 192, 193]. These differences pose substantial barriers to effective information integration. During practical spatiotemporal fusion operations, even spectrally similar images generate unavoidable pixel-level disparities due to variations in spatial resolution, band width, and atmospheric interference. With the recent emergence of drone technology, attempts to merge drone imagery with satellite imagery have increased. However, the spatial scale and observational condition differences between these cross-scale images far exceed those among data from similar platforms, further intensifying the complexity of multi-source heterogeneous data fusion [6, 13]. Addressing the proper integration of multi-modal, multi-scale data has become an urgent challenge in remote sensing data processing tasks.

3.5. Computational Efficiency

In practical applications, spatiotemporal fusion technology faces data processing speed bottlenecks [33]. Most fusion methods rely on pixel-level calculations or moving window strategies, which, though accurate, are too slow. For large-scale imagery, personal computers can take hours to a full day, which is adequate for small-scale areas but insufficient for larger regions or global tasks [13]. To improve efficiency, two strategies are used: optimizing computational unit granularity to balance pixel-level and image-level calculations, and employing more efficient frameworks like GPU parallel acceleration or cloud computing [6, 13]. However, practical issues such as platform resource costs and data management stability still limit speed improvements. Ongoing efforts are needed to enhance the computational efficiency and real-time performance of fusion algorithms for large-scale data.

4. Opportunities

4.1. Balancing Data- and Model-driven Methods

Balancing data-driven and model-driven approaches stems from different emphases on generalization and precision in remote sensing image processing. As mentioned before, generalization refers to a model's ability to perform well on unfamiliar training data, essentially its adaptability or transferability [13]. Precision measures how well a model's predictions match actual results when processing known data. Data-driven methods like deep learning demonstrate exceptional self-adaptive capabilities, excelling at extracting complex non-linear features from remote sensing imagery, yet heavily depend on data scale and diversity. When datasets lack sufficient coverage, data-driven methods experience a significant decline in generalization ability for unknown scenarios. This leads to an unacceptable risk in practical remote sensing applications. Conversely, model-driven approaches provide deeper understanding of the physical mechanisms behind imaging processes and exhibit stable generalization performance, but struggle with complex non-linear relationships in remote sensing images. Combining data-driven and model-driven methods represents a popular coupling approach that reduces deep learning networks' dependence on large-scale data while enhancing model interpretability and generalizability. For instance, in synthetic aperture radar (SAR) image despeckle tasks, variational models constrain deep networks, aligning learning processes with actual physical characteristics [194]. In hyperspectral image denoising, embedding model-driven constraints into network structures maintains effective generalization capabilities even with incomplete data [194, 195]. Nevertheless, the complexity and diversity of remote sensing data, coupled with inherent limitations in model-driven approaches' modeling capabilities, means this coupling technology rarely achieves optimal performance in practical applications. The form and degree of integration still require exploration and optimization by researchers.

4.2. Few-shot Learning and Unsupervised Learning

When annotated data lacks comprehensiveness, deep learning methods cannot be effectively generalized. Particularly for spatiotemporal fusion, there is a critical lack of large-scale datasets. Few-shot learning and unsupervised learning excel precisely under these circumstances. Few-shot learning's transfer learning and meta-learning mechanisms thoroughly explore potential relationships between high and low-resolution images, enhancing model performance when data is scarce. In land cover classification tasks, few-shot learning methods can utilize small amounts of labeled high-resolution data to adapt models to low-resolution image environments, enabling more accurate cross-scale classification. In situations where remote sensing data is difficult to acquire or existing samples lack cleanliness, unsupervised learning proves valuable as it completely eliminates dependence on labeled data. A typical approach leverages GAN's unique adversarial loss and competitive training mechanism to capture high-level abstract features when reference images are insufficiently clean, achieving high-quality image restoration tasks [196]. Researchers can subsequently focus on integrating remote sensing observation models with unsupervised network structures, enhancing the robustness and generalization of corresponding methods to achieve more stable and reliable spatiotemporal fusion technology [196, 197].

4.3. Potential of Multi-task Learning

Multi-task Learning (MTL) offers the core advantage of effectively integrating associated features between multiple tasks, thereby improving overall processing efficiency and accuracy. This characteristic aligns perfectly with several remote sensing image processing requirements. For instance, remote sensing image fusion frequently encounters distribution feature differences caused by seasonal changes, while MTL can alleviate accuracy losses resulting from insufficient feature migration by sharing information between different tasks. When high-quality paired samples are scarce, MTL can also leverage its characteristics to address such data scarcity issues [198]. In practical applications, MTL can configure image fusion tasks from different periods as a group of interconnected subtasks sharing feature spaces, achieving personalized processing of individual tasks while utilizing task synergies to enhance overall fusion performance. For example, treating the fusion of Landsat and MODIS images from different time points as interconnected prediction tasks effectively captures the continuity of seasonal changes and spatial details, enhancing spatiotemporal consistency in fused images [198, 199]. Looking forward, researchers can further enhance model generalization and robustness by integrating MTL with deep learning frameworks, improving both processing efficiency and prediction accuracy.

4.4. Foundation Models for Spatiotemporal Fusion

Remote sensing foundation models (RSFMs) can integrate multi-source, multi-temporal, and multi-resolution remote sensing data through a unified framework to generate surface observation data with high spatial continuity,

showing potential for spatiotemporal fusion tasks [200]. SatMAE [201] can capture spatiotemporal dependencies in multispectral images through temporal mask reconstruction pretraining, effectively combining high and low-resolution images from different time periods. Scale-MAE [202] enhances detail consistency by combining multi-scale reconstruction and land feature distance encoding, fusing remote sensing data from different sensors. CROMA [203] extracts invariant spatiotemporal features through cross-modal contrastive learning, thereby analyzing heterogeneous data sources. Generative models similar to DiffusionSat [204] can utilize diffusion processes to reconstruct continuous dynamic land cover, cloud-contaminated or missing temporal images for practical applications. RSFMs are suitable for large-scale spatiotemporal analysis and can resolve spatiotemporal conflicts caused by sensor differences through multi-modal alignment capabilities, certainly applicable to specific spatiotemporal fusion tasks in the future [200].

5. Conclusion

With the rapid advancement of deep learning technologies, remote sensing spatiotemporal fusion has achieved remarkable progress in model performance, data processing capabilities, and application scenarios. This review systematically examines the principal research achievements in this field, encompassing network architectures, datasets with evaluation metrics, research challenges, and future opportunities. Deep learning-driven remote sensing spatiotemporal fusion technology currently experiences accelerated development and holds vast potential. The collaboration between industry and academia will further catalyze growth in this sector while providing robust technical support for addressing global environmental issues, resource management, and disaster-related problems. We hope this review provides valuable insights and a solid foundation for researchers and practitioners in the field, facilitating their future explorations and innovations in remote sensing spatiotemporal fusion technologies.

Declaration of Competing Interest

The authors declare that they have no known competing financial interests or personal relationships that could have appeared to influence the work reported in this paper.

References

- [1] C. Feichtenhofer, A. Pinz, A. Zisserman, Convolutional Two-Stream Network Fusion for Video Action Recognition, in: *IEEE Conf. Comput. Vis. Pattern Recog.*, IEEE, Las Vegas, NV, USA, 2016, pp. 1933–1941. doi:10.1109/CVPR.2016.213.
- [2] K. Niu, H. Zhang, T. Zhou, C. Cheng, C. Wang, A Novel spatiotemporal Model for City-Scale Traffic Speed Prediction, *IEEE Access* 7 (2019) 30050–30057.
- [3] J. Dafni Rose, K. Jaspin, K. Vijayakumar, Lung Cancer Diagnosis Based on Image Fusion and Prediction Using CT and PET Image, in: E. Priya, V. Rajinikanth (Eds.), *Signal and Image Processing Techniques for the Development of Intelligent Healthcare*

- Systems*, Springer Singapore, Singapore, 2021, pp. 67–86. doi:10.1007/978-981-15-6141-2_4.
- [4] Z. Tan, M. Gao, X. Li, L. Jiang, A Flexible Reference-Insensitive Spatiotemporal Fusion Model for Remote Sensing Images Using Conditional Generative Adversarial Network, *IEEE Trans. Geosci. Remote Sens.* 60 (2022) 1–13.
- [5] P. Liu, J. Li, L. Wang, G. He, Remote Sensing Data Fusion With Generative Adversarial Networks: State-of-the-art Methods and Future Research Directions, *IEEE Geosci. Remote Sens. Mag.* 10 (2022) 295–328.
- [6] M. Belgiu, A. Stein, Spatiotemporal Image Fusion in Remote Sensing, *Remote Sens.* 11 (2019) 818.
- [7] J. Walterskirchen, S. Häffner, C. Oswald, M. N. Binetti, Taking Time Seriously: Predicting Conflict Fatalities Using Temporal Fusion Transformers, 2024. doi:10.31235/osf.io/7xu93.
- [8] X. Zhu, J. Chen, F. Gao, X. Chen, J. G. Masek, An Enhanced Spatial and Temporal Adaptive Reflectance Fusion Model for Complex Heterogeneous Regions, *Remote Sens. Environ.* 114 (2010) 2610–2623.
- [9] J. Xiao, A. Aggarwal, N. Duc, A. Arya, U. Rage, R. Avtar, A review of remote sensing image spatiotemporal fusion: Challenges, applications and recent trends, *Remote Sens. Appl. Soc. Environ.* 32 (2023) 101005.
- [10] A. Li, Y. Bo, Y. Zhu, P. Guo, J. Bi, Y. He, Blending Multi-resolution Satellite Sea Surface Temperature (SST) Products Using Bayesian Maximum Entropy Method, *Remote Sens. Environ.* 135 (2013) 52–63.
- [11] B. Huang, H. Zhang, H. Song, J. Wang, C. Song, Unified Fusion of Remote-sensing Imagery: Generating Simultaneously High-Resolution Synthetic Spatial–Temporal–Spectral Earth Observations, *Remote Sens. Lett.* 4 (2013) 561–569.
- [12] J. Li, Y. Li, L. He, J. Chen, A. Plaza, spatiotemporal Fusion for Remote Sensing Data: An Overview and New Benchmark, *Sci. China Inf. Sci.* 63 (2020) 140301.
- [13] X. Zhu, F. Cai, J. Tian, T. Williams, Spatiotemporal Fusion of Multisource Remote Sensing Data: Literature Survey, Taxonomy, Principles, Applications, and Future Directions, *Remote Sens.* 10 (2018) 527.
- [14] X. Jiang, B. Huang, Unmixing-Based Spatiotemporal Image Fusion Accounting for Complex Land Cover Changes, *IEEE Trans. Geosci. Remote Sens.* 60 (2022) 1–10.
- [15] B. Huang, H. Zhang, spatiotemporal reflectance fusion via unmixing: Accounting for both phenological and land-cover changes, *Int. J. Remote Sens.* 35 (2014) 6213–6233.
- [16] B. Zhukov, D. Oertel, F. Lanzl, G. Reinhackel, Unmixing-based Multisensor Multiresolution Image Fusion, *IEEE Trans. Geosci. Remote Sens.* 37 (1999) 1212–1226.
- [17] B. Huang, X. Jiang, An enhanced unmixing model for spatiotemporal image fusion, *Natl. Remote Sens. Bull.* (2021).
- [18] B. Huang, H. Song, Spatiotemporal Reflectance Fusion via Sparse Representation, *IEEE Trans. Geosci. Remote Sens.* 50 (2012) 3707–3716.
- [19] X. Liu, C. Deng, S. Wang, G.-B. Huang, B. Zhao, P. Lauren, Fast and Accurate Spatiotemporal Fusion Based Upon Extreme Learning Machine, *IEEE Geosci. Remote Sens. Lett.* 13 (2016) 2039–2043.
- [20] F. Gao, J. Masek, M. Schwaller, F. Hall, On the Blending of the Landsat and MODIS Surface Reflectance: Predicting Daily Landsat Surface Reflectance, *IEEE Trans. Geosci. Remote Sens.* 44 (2006) 2207–2218.
- [21] X. Zhu, J. Chen, F. Gao, X. Chen, J. G. Masek, An Enhanced Spatial and Temporal Adaptive Reflectance Fusion Model for Complex Heterogeneous Regions, *Remote Sens. Environ.* 114 (2010) 2610–2623.
- [22] T. Hilker, M. A. Wulder, N. C. Coops, J. Linke, G. McDermid, J. G. Masek, F. Gao, J. C. White, A New Data Fusion Model for High Spatial- and Temporal-Resolution Mapping of Forest Disturbance Based on Landsat and MODIS, *Remote Sens. Environ.* 113 (2009) 1613–1627.

- [23] X. Zhu, E. H. Helmer, F. Gao, D. Liu, J. Chen, M. A. Lefsky, A Flexible Spatiotemporal Method for Fusing Satellite Images with Different Resolutions, *Remote Sens. Environ.* 172 (2016) 165–177.
- [24] Q. Wang, P. M. Atkinson, spatiotemporal Fusion for Daily Sentinel-2 Images, *Remote Sens. Environ.* 204 (2018) 31–42.
- [25] P. Wu, H. Shen, L. Zhang, F.-M. Göttsche, Integrated Fusion of Multi-Scale Polar-Orbiting and Geostationary Satellite Observations for the Mapping of High Spatial and Temporal Resolution Land Surface Temperature, *Remote Sens. Environ.* 156 (2015) 169–181.
- [26] J. Li, D. Hong, L. Gao, J. Yao, K. Zheng, B. Zhang, J. Chanussot, Deep Learning in Multimodal Remote Sensing Data Fusion: A Comprehensive Review, *Int. J. Appl. Earth Obs. Geoinf.* 112 (2022) 102926.
- [27] M. Jiang, H. Shao, A CNN-Transformer Combined Remote Sensing Imagery Spatiotemporal Fusion Model, *IEEE J. Sel. Top. Appl. Earth Obs. Remote Sens.* 17 (2024) 13995–14009.
- [28] A. Krizhevsky, I. Sutskever, G. E. Hinton, ImageNet Classification with Deep Convolutional Neural Networks, in: *Adv. Neural Inf. Process. Syst.*, volume 25, Curran Associates, Inc., 2012.
- [29] I. Goodfellow, J. Pouget-Abadie, M. Mirza, B. Xu, D. Warde-Farley, S. Ozair, A. Courville, Y. Bengio, Generative Adversarial Nets, in: *Adv. Neural Inf. Process. Syst.*, volume 27, Curran Associates, Inc., 2014.
- [30] M. Arjovsky, S. Chintala, L. Bottou, Wasserstein Generative Adversarial Networks, in: *Proc. 34th Int. Conf. Mach. Learn.*, PMLR, 2017, pp. 214–223.
- [31] A. Vaswani, N. Shazeer, N. Parmar, J. Uszkoreit, L. Jones, A. N. Gomez, L. Kaiser, I. Polosukhin, Attention Is All You Need, 2023. doi:10.48550/arXiv.1706.03762. arXiv:1706.03762.
- [32] J. Xiao, A. K. Aggarwal, N. H. Duc, A. Arya, U. K. Rage, R. Avatar, A Review of Remote Sensing Image Spatiotemporal Fusion: Challenges, Applications and Recent Trends, *Remote Sens. Appl. Soc. Environ.* 32 (2023) 101005.
- [33] P. Wu, Z. Yin, C. Zeng, S.-B. Duan, F.-M. Göttsche, X. Ma, X. Li, H. Yang, H. Shen, Spatially Continuous and High-Resolution Land Surface Temperature Product Generation: A Review of Reconstruction and Spatiotemporal Fusion Techniques, *IEEE Geosci. Remote Sens. Mag.* 9 (2021) 112–137.
- [34] H. Huang, W. He, H. Zhang, Y. Xia, L. Zhang, STFDiff: Remote Sensing Image Spatiotemporal Fusion with Diffusion Models, *Inf. Fusion.* 111 (2024).
- [35] S. Wang, F. Fan, STINet: Vegetation Changes Reconstruction Through a Transformer-Based Spatiotemporal Fusion Approach in Remote Sensing, *IEEE Trans. Geosci. Remote Sens.* 62 (2024) 1–16.
- [36] C. Weng, Y. Zhan, X. Gu, J. Yang, Y. Liu, H. Guo, Z. Lian, S. Zhang, Z. Wang, X. Zhao, The Spatially Seamless Spatiotemporal Fusion Model Based on Generative Adversarial Networks, *IEEE J. Sel. Top. Appl. Earth Obs. Remote Sens.* 17 (2024) 12760–12771.
- [37] J. Mu, J. Yang, C. Wang, Y. Jia, Spatiotemporal Fusion Network Based on Improved Transformer for Inverting Subsurface Thermohaline Structure, *IEEE Trans. Geosci. Remote Sens.* 62 (2024).
- [38] Y. Xie, J. Hu, K. He, L. Cao, K. Yang, L. Chen, The Gan Spatiotemporal Fusion Model Based on Multi-Scale Convolution and Attention Mechanism for Remote Sensing Images, *IEEE J. Sel. Top. Appl. Earth Obs. Remote Sens.* (2024) 1–13.
- [39] Z. Xu, H. Sun, T. Zhang, H. Xu, D. Wu, J. Gao, The High Spatial Resolution Drought Response Index (HiDRI): An Integrated Framework for Monitoring Vegetation Drought with Remote Sensing, Deep Learning, and Spatiotemporal Fusion, *Remote Sens. Environ.* 312 (2024).
- [40] Y. Zhang, P. Wang, K. Tansey, M. Li, F. Guo, J. Liu, S. Zhang, Spatiotemporal Data Fusion of Index-Based VTCI Using Sentinel-2 and -3 Satellite Data for Field-Scale Drought Monitoring, *IEEE Trans. Geosci. Remote Sens.* 62 (2024) 1–15.
- [41] T. Jia, G. Cheng, Z. Chen, J. Yang, Y. Li, Forecasting Urban Air Pollution Using Multi-Site Spatiotemporal Data Fusion Method (Geo-BiLSTMA), *Atmos. Pollut. Res.* 15 (2024) 102107.
- [42] Y. Cui, P. Liu, Y. Ma, L. Chen, M. Xu, X. Guo, Pansharpening via Predictive Filtering with Element-Wise Feature Mixing, *ISPRS J. Photogramm. Remote Sens.* 219 (2025) 22–37.
- [43] X. Zhang, S. Li, Z. Tan, X. Li, Enhanced Wavelet Based Spatiotemporal Fusion Networks Using Cross-Paired Remote Sensing Images, *ISPRS J. Photogramm. Remote Sens.* 211 (2024) 281–297.
- [44] Z. Ao, Y. Sun, X. Pan, Q. Xin, Deep Learning-Based Spatiotemporal Data Fusion Using a Patch-to-Pixel Mapping Strategy and Model Comparisons, *IEEE Trans. Geosci. Remote Sens.* 60 (2022) 1–18.
- [45] H. Song, Q. Liu, G. Wang, R. Hang, B. Huang, Spatiotemporal Satellite Image Fusion Using Deep Convolutional Neural Networks, *IEEE J. Sel. Top. Appl. Earth Obs. Remote Sens.* 11 (2018) 821–829.
- [46] D. Lei, Q. Zhu, Y. Li, J. Tan, S. Wang, T. Zhou, L. Zhang, HPLTS-GAN: A High-Precision Remote Sensing Spatiotemporal Fusion Method Based on Low Temporal Sensitivity, *IEEE Trans. Geosci. Remote Sens.* 62 (2024) 1–16.
- [47] Y. Ma, Q. Wang, J. Wei, Spatiotemporal Fusion via Conditional Diffusion Model, *IEEE Geosci. Remote Sens. Lett.* 21 (2024) 1–5.
- [48] S. Chen, J. Wang, P. Gong, ROBOT: A Spatiotemporal Fusion Model toward Seamless Data Cube for Global Remote Sensing Applications, *Remote Sens. Environ.* 294 (2023) 113616.
- [49] H. Guo, D. Ye, H. Xu, L. Bruzzone, OBSUM: An Object-Based Spatial Unmixing Model for Spatiotemporal Fusion of Remote Sensing Images, *Remote Sens. Environ.* 304 (2024) 114046.
- [50] J. Kim, T. Kim, J.-G. Ryu, Multi-Source Deep Data Fusion and Super-Resolution for Downscaling Sea Surface Temperature Guided by Generative Adversarial Network-Based Spatiotemporal Dependency Learning, *Int. J. Appl. Earth Obs. Geoinf.* 119 (2023) 103312.
- [51] H. Wu, Q. Yang, J. Liu, G. Wang, A Spatiotemporal Deep Fusion Model for Merging Satellite and Gauge Precipitation in China, *J. Hydrol.* 584 (2020) 124664.
- [52] Y. Gu, J. Chen, Z. Chen, M. Li, S. Zhu, Y. P. Wang, Near Real-Time Monitoring of Muddy Intertidal Zones Based on Spatiotemporal Fusion of Optical Satellites Data, *IEEE J. Sel. Top. Appl. Earth Obs. Remote Sens.* 17 (2024) 1596–1609.
- [53] Y. Zhang, R. Fan, P. Duan, J. Dong, Z. Lei, DCDGAN-STF: A Multiscale Deformable Convolution Distillation GAN for Remote Sensing Image Spatiotemporal Fusion, *IEEE J. Sel. Top. Appl. Earth Obs. Remote Sens.* 17 (2024) 19436–19450.
- [54] W. Chen, X. Hao, W. Yuankai, Y. Liang, Terra: A Multimodal spatiotemporal Dataset Spanning the Earth, in: *The Thirty-Eight Conference on Neural Information Processing Systems Datasets and Benchmarks Track*, 2024.
- [55] J. Zhao, M. Zhang, Z. Zhou, Z. Wang, F. Lang, H. Shi, N. Zheng, CFFormer: A Cross-Fusion Transformer Framework for the Semantic Segmentation of Multisource Remote Sensing Images, *IEEE Trans. Geosci. Remote Sens.* 63 (2025) 1–17.
- [56] C. Yu, F. Wang, Y. Wang, Z. Shao, T. Sun, D. Yao, Y. Xu, MGSFormer: A Multi-Granularity Spatiotemporal Fusion Transformer for Air Quality Prediction, *Inf. Fusion.* 113 (2025) 102607.
- [57] T. Kattenborn, J. Leitloff, F. Schiefer, S. Hinz, Review on Convolutional Neural Networks (CNN) in Vegetation Remote Sensing, *ISPRS J. Photogramm. Remote Sens.* 173 (2021) 24–49.
- [58] A. Zhao, M. Qin, S. Wu, R. Liu, Z. Du, ENSO Forecasts With Spatiotemporal Fusion Transformer Network, *IEEE J. Sel. Top. Appl. Earth Obs. Remote Sens.* 17 (2024) 17066–17074.
- [59] S. Sun, L. Mu, L. Wang, P. Liu, L-UNet: An LSTM Network for Remote Sensing Image Change Detection, *IEEE Geosci. Remote Sens. Lett.* 19 (2022) 1–5.
- [60] W. Shi, R. Rajkumar, Point-GNN: Graph Neural Network for 3D Object Detection in a Point Cloud, in: *IEEE Conf. Comput. Vis. Pattern Recog.*, IEEE, Seattle, WA, USA, 2020, pp. 1708–1716. doi:10.1109/CVPR42600.2020.00178.
- [61] K. Sun, Y. Tian, DBFNet: A Dual-Branch Fusion Network for Underwater Image Enhancement, *Remote Sens.* 15 (2023) 1195.

- [62] G. Chen, H. Lu, D. Di, L. Li, M. Emam, W. Jing, StfMLP: Spatiotemporal Fusion Multilayer Perceptron for Remote-Sensing Images, *IEEE Geosci. Remote Sens. Lett.* 20 (2023).
- [63] X. Liu, C. Deng, J. Chanussot, D. Hong, B. Zhao, StfNet: A Two-Stream Convolutional Neural Network for Spatiotemporal Image Fusion, *IEEE Trans. Geosci. Remote Sens.* 57 (2019) 6552–6564.
- [64] Z. Tan, L. Di, M. Zhang, L. Guo, M. Gao, An Enhanced Deep Convolutional Model for Spatiotemporal Image Fusion, *Remote Sens.* 11 (2019).
- [65] M. Peng, L. Zhang, X. Sun, Y. Cen, X. Zhao, A Fast Three-Dimensional Convolutional Neural Network-Based Spatiotemporal Fusion Method (STF3DCNN) Using a Spatial-Temporal-Spectral Dataset, *Remote Sens.* 12 (2020) 3888.
- [66] Z. Yin, P. Wu, G. M. Foody, Y. Wu, Z. Liu, Y. Du, F. Ling, Spatiotemporal Fusion of Land Surface Temperature Based on a Convolutional Neural Network, *IEEE Trans. Geosci. Remote Sens.* 59 (2021) 1808–1822.
- [67] W. Li, C. Yang, Y. Peng, X. Zhang, A Multi-Cooperative Deep Convolutional Neural Network for Spatiotemporal Satellite Image Fusion, *IEEE J. Sel. Top. Appl. Earth Obs. Remote Sens.* 14 (2021) 10174–10188.
- [68] J. Wei, W. Tang, C. He, Enblending Mosaicked Remote Sensing Images With Spatiotemporal Fusion of Convolutional Neural Networks, *IEEE J. Sel. Top. Appl. Earth Obs. Remote Sens.* 14 (2021) 5891–5902.
- [69] P. Qin, H. Huang, H. Tang, J. Wang, C. Liu, MUSTFN: A Spatiotemporal Fusion Method for Multi-Scale and Multi-Sensor Remote Sensing Images Based on a Convolutional Neural Network, *Int. J. Appl. Earth Obs. Geoinf.* 115 (2022).
- [70] F. Cheng, Z. Fu, B. Tang, L. Huang, K. Huang, X. Ji, STF-EGFA: A Remote Sensing Spatiotemporal Fusion Network with Edge-Guided Feature Attention, *Remote Sens.* 14 (2022) 3057.
- [71] Z. Zhu, Y. Tao, X. Luo, HCNNet: A Hybrid Convolutional Neural Network for Spatiotemporal Image Fusion, *IEEE Trans. Geosci. Remote Sens.* 60 (2022).
- [72] Y. Chen, Y. Ge, Spatiotemporal Image Fusion Using Multiscale Attention-Aware Two-Stream Convolutional Neural Networks, *Sci. Remote Sens.* 6 (2022).
- [73] H. Jiang, Y. Qian, G. Yang, H. Liu, MLKNet: Multi-Stage for Remote Sensing Image Spatiotemporal Fusion Network Based on a Large Kernel Attention, *IEEE J. Sel. Top. Appl. Earth Obs. Remote Sens.* 17 (2024) 1257–1268.
- [74] D. Cui, S. Wang, C. Zhao, H. Zhang, A Novel Remote Sensing Spatiotemporal Data Fusion Framework Based on the Combination of Deep-Learning Downscaling and Traditional Fusion Algorithm, *IEEE J. Sel. Top. Appl. Earth Obs. Remote Sens.* 17 (2024) 7957–7970.
- [75] G. Chen, P. Jiao, Q. Hu, L. Xiao, Z. Ye, SwinSTFM: Remote Sensing Spatiotemporal Fusion Using Swin Transformer, *IEEE Trans. Geosci. Remote Sens.* 60 (2022) 1–18.
- [76] B. Song, P. Liu, J. Li, L. Wang, L. Zhang, G. He, L. Chen, J. Liu, MLFF-GAN: A Multilevel Feature Fusion With GAN for Spatiotemporal Remote Sensing Images, *IEEE Trans. Geosci. Remote Sens.* 60 (2022) 1–16.
- [77] Z. Cui, J. Zhang, G. Noh, H. J. Park, MFDGCN: Multi-Stage spatiotemporal Fusion Diffusion Graph Convolutional Network for Traffic Prediction, *Appl. Sci.* 12 (2022) 2688.
- [78] J. Wei, L. Gan, W. Tang, M. Li, Y. Song, Diffusion Models for spatiotemporal-Spectral Fusion of Homogeneous Gaofen-1 Satellite Platforms, *Int. J. Appl. Earth Obs. Geoinf.* 128 (2024) 103752.
- [79] H. Cui, L. Chai, H. Li, S. Zhao, Spatiotemporal Fusion of Soil Freeze/Thaw Datasets at Decision-Level Based on Convolutional Long Short-Term Memory Network, in: *IEEE Int. Geosci. Remote Sens. Symp.*, IEEE, Athens, Greece, 2024, pp. 8983–8986. doi:10.1109/IGARSS53475.2024.10641699.
- [80] J. Wang, W. Wang, W. Yu, X. Liu, K. Jia, X. Li, M. Zhong, Y. Sun, Y. Xu, STHGCN: A Spatiotemporal Prediction Framework Based on Higher-Order Graph Convolution Networks, *Knowl.-Based Syst.* 258 (2022) 109985.
- [81] G. Yang, Y. Qian, H. Liu, B. Tang, R. Qi, Y. Lu, J. Geng, MSFusion: Multistage for Remote Sensing Image Spatiotemporal Fusion Based on Texture Transformer and Convolutional Neural Network, *IEEE J. Sel. Top. Appl. Earth Obs. Remote Sens.* 15 (2022) 4653–4666.
- [82] Z. Cai, Q. Hu, X. Zhang, J. Yang, H. Wei, J. Wang, Y. Zeng, G. Yin, W. Li, L. You, B. Xu, Z. Shi, Improving Agricultural Field Parcel Delineation with a Dual Branch Spatiotemporal Fusion Network by Integrating Multimodal Satellite Data, *ISPRS J. Photogramm. Remote Sens.* 205 (2023) 34–49.
- [83] P. Liu, L. Wang, J. Chen, Y. Cui, Semiblind Compressed Sensing: A Bidirectional-Driven Method for Spatiotemporal Fusion of Remote Sensing Images, *IEEE J. Sel. Top. Appl. Earth Obs. Remote Sens.* 17 (2024) 19048–19066.
- [84] Z. Li, F. Liu, W. Yang, S. Peng, J. Zhou, A Survey of Convolutional Neural Networks: Analysis, Applications, and Prospects, *IEEE Trans. Neural Netw. Learn. Syst.* 33 (2022) 6999–7019.
- [85] E. Maggiori, Y. Tarabalka, G. Charpiat, P. Alliez, Convolutional Neural Networks for Large-Scale Remote-Sensing Image Classification, *IEEE Trans. Geosci. Remote Sens.* 55 (2017) 645–657.
- [86] Y. Sun, B. Xue, M. Zhang, G. G. Yen, Evolving Deep Convolutional Neural Networks for Image Classification, 2019. doi:10.48550/arXiv.1710.10741. arXiv:1710.10741.
- [87] U. Muhammad, W. Wang, S. P. Chattha, S. Ali, Pre-Trained VGGNet Architecture for Remote-Sensing Image Scene Classification, in: *Int. Conf. Pattern Recogn.*, IEEE, Beijing, 2018, pp. 1622–1627. doi:10.1109/ICPR.2018.8545591.
- [88] K. Simonyan, A. Zisserman, Very Deep Convolutional Networks for Large-Scale Image Recognition, 2015. doi:10.48550/arXiv.1409.1556. arXiv:1409.1556.
- [89] Y. Li, J. Li, L. He, J. Chen, A. Plaza, A New Sensor Bias-driven spatiotemporal Fusion Model Based on Convolutional Neural Networks, *Sci. China Inf. Sci.* 63 (2020) 140302.
- [90] Z. Tan, M. Gao, J. Yuan, L. Jiang, H. Duan, A Robust Model for MODIS and Landsat Image Fusion Considering Input Noise, *IEEE Trans. Geosci. Remote Sens.* 60 (2022).
- [91] S. Woo, J. Park, J.-Y. Lee, I. S. Kweon, CBAM: Convolutional block attention module, in: *Proceedings of the European conference on computer vision (ECCV)*, 2018, pp. 3–19.
- [92] J. Cai, B. Huang, T. Fung, Progressive Spatiotemporal Image Fusion with Deep Neural Networks, *Int. J. Appl. Earth Obs. Geoinf.* 108 (2022) 102745.
- [93] Y.-Z. Chen, T.-J. Liu, K.-H. Liu, Super-Resolution of Satellite Images by Two-Dimensional RRDB and Edge-Enhancement Generative Adversarial Network, in: *ICASSP 2022 - 2022 IEEE International Conference on Acoustics, Speech and Signal Processing (ICASSP)*, 2022, pp. 1825–1829. doi:10.1109/ICASSP43922.2022.9747063.
- [94] M. You, X. Meng, Q. Liu, F. Shao, R. Fu, CIG-STF: Change Information Guided Spatiotemporal Fusion for Remote Sensing Images, *IEEE Trans. Geosci. Remote Sens.* 62 (2024).
- [95] Z. Lian, Y. Zhan, W. Zhang, Z. Wang, W. Liu, X. Huang, Recent Advances in Deep Learning-Based Spatiotemporal Fusion Methods for Remote Sensing Images, *Sensors* 25 (2025) 1093.
- [96] D. Jia, C. Cheng, S. Shen, L. Ning, Multitask Deep Learning Framework for Spatiotemporal Fusion of NDVI, *IEEE Trans. Geosci. Remote Sens.* 60 (2022) 1–13.
- [97] P. Arun, K. Buddhiraju, A. Porwal, J. Chanussot, CNN Based Spectral Super-Resolution of Remote Sensing Images, *Signal Processing* 169 (2020) 107394.
- [98] W. Li, C. Yang, Y. Peng, J. Du, A Pseudo-Siamese Deep Convolutional Neural Network for Spatiotemporal Satellite Image Fusion, *IEEE J. Sel. Top. Appl. Earth Obs. Remote Sens.* 15 (2022) 1205–1220.
- [99] X. Wang, X. Wang, Spatiotemporal Fusion of Remote Sensing Image Based on Deep Learning, *Journal of Sensors* 2020 (2020) 8873079.
- [100] Q. Wang, B. Li, T. Xiao, J. Zhu, C. Li, D. F. Wong, L. S. Chao, Learning Deep Transformer Models for Machine Translation, 2019. doi:10.48550/arXiv.1906.01787. arXiv:1906.01787.

- [101] S. Karita, N. Chen, T. Hayashi, T. Hori, H. Inaguma, Z. Jiang, M. Someki, N. E. Y. Soplin, R. Yamamoto, X. Wang, S. Watanabe, T. Yoshimura, W. Zhang, A Comparative Study on Transformer vs RNN in Speech Applications, in: 2019 IEEE Automatic Speech Recognition and Understanding Workshop (ASRU), 2019, pp. 449–456. doi:10.1109/ASRU46091.2019.9003750. arXiv:1909.06317.
- [102] Z. Wang, Y. Ma, Z. Liu, J. Tang, R-Transformer: Recurrent Neural Network Enhanced Transformer, 2019. doi:10.48550/arXiv.1907.05572. arXiv:1907.05572.
- [103] A. Gillioz, J. Casas, E. Mugellini, O. A. Khaled, Overview of the Transformer-Based Models for NLP Tasks, in: 2020 Federated Conference on Computer Science and Information Systems, 2020, pp. 179–183. doi:10.15439/2020F20.
- [104] A. Jamshed, M. M. Fraz, NLP Meets Vision for Visual Interpretation - A Retrospective Insight and Future Directions, in: 2021 International Conference on Digital Futures and Transformative Technologies (ICoDT2), 2021, pp. 1–8. doi:10.1109/ICoDT252288.2021.9441517.
- [105] X. Chen, H. Xie, X. Tao, Vision, Status, and Research Topics of Natural Language Processing, *Natural Lang. Process. J. 1* (2022) 100001.
- [106] A. Dosovitskiy, L. Beyer, A. Kolesnikov, D. Weissenborn, X. Zhai, T. Unterthiner, M. Dehghani, M. Minderer, G. Heigold, S. Gelly, J. Uszkoreit, N. Houlsby, An Image Is Worth 16x16 Words: Transformers for Image Recognition at Scale, 2021. doi:10.48550/arXiv.2010.11929. arXiv:2010.11929.
- [107] J. Sun, B. Wu, T. Zhao, L. Gao, K. Xie, T. Lin, J. Sui, X. Li, X. Wu, X. Ni, Classification for Thyroid Nodule Using ViT with Contrastive Learning in Ultrasound Images, *Comput. Biol. Med.* 152 (2023) 106444.
- [108] G.-I. Kim, K. Chung, ViT-Based Multi-Scale Classification Using Digital Signal Processing and Image Transformation, *IEEE Access* 12 (2024) 58625–58638.
- [109] A. Safaei, M. Riazi, S. Shariat, A Novel Experimental-Theoretical Method to Improve MMP Estimation Using ViT Technique, *J Pet Sci Eng* 220 (2023) 111182.
- [110] E. Şahin, D. Özdemir, H. Temurtaş, Multi-Objective Optimization of ViT Architecture for Efficient Brain Tumor Classification, *Biomed. Signal Process. Control* 91 (2024) 105938.
- [111] A. A. Aleissae, A. Kumar, R. M. Anwer, S. Khan, H. Cholakkal, G.-S. Xia, F. S. Khan, Transformers in Remote Sensing: A Survey, *Remote Sens.* 15 (2023) 1860.
- [112] R. Wang, L. Ma, G. He, B. A. Johnson, Z. Yan, M. Chang, Y. Liang, Transformers for Remote Sensing: A Systematic Review and Analysis, *Sensors* 24 (2024) 3495.
- [113] Y. Bazi, L. Bashmal, M. M. A. Rahhal, R. A. Dayil, N. A. Ajlan, Vision Transformers for Remote Sensing Image Classification, *Remote Sens.* 13 (2021) 516.
- [114] Y. Ma, H. Wu, L. Wang, B. Huang, R. Ranjan, A. Zomaya, W. Jie, Remote Sensing Big Data Computing: Challenges and Opportunities, *Future Gener. Comput. Syst.* 51 (2015) 47–60.
- [115] M. Chi, A. Plaza, J. A. Benediktsson, Z. Sun, J. Shen, Y. Zhu, Big Data for Remote Sensing: Challenges and Opportunities, *Proc. IEEE* 104 (2016) 2207–2219.
- [116] J. Guo, N. Jia, J. Bai, Transformer Based on Channel-Spatial Attention for Accurate Classification of Scenes in Remote Sensing Image, *Sci. Rep.* 12 (2022) 15473.
- [117] S. Liang, Z. Hua, J. Li, Enhanced Self-Attention Network for Remote Sensing Building Change Detection, *IEEE J. Sel. Top. Appl. Earth Obs. Remote Sens.* 16 (2023) 4900–4915.
- [118] M. Qi, Q. Wang, S. Zhuang, K. Zhang, K. Li, Y. Liu, Y. Yang, Exploring Reliable Infrared Object Tracking with spatiotemporal Fusion Transformer, *Knowl.-Based Syst.* 284 (2024) 111234.
- [119] S. Wang, Y. Lin, Y. Jia, J. Sun, Z. Yang, Unveiling the Multi-Dimensional spatiotemporal Fusion Transformer (MDSTFT): A Revolutionary Deep Learning Framework for Enhanced Multi-Variate Time Series Forecasting, *IEEE Access* 12 (2024) 115895–115904.
- [120] L. Wang, M. Cao, Y. Zhong, X. Yuan, Spatial-Temporal Transformer for Video Snapshot Compressive Imaging, *IEEE Trans. Pattern Anal. Mach. Intell.* 45 (2023) 9072–9089.
- [121] Z. Chen, J. Jin, J. Pan, spatiotemporal Swin Transformer-Based 4-D EEG Emotion Recognition, in: 2023 IEEE International Conference on Bioinformatics and Biomedicine (BIBM), 2023, pp. 1850–1855. doi:10.1109/BIBM58861.2023.10385526.
- [122] P. Wang, Z. He, B. Huang, M. D. Mura, H. Leung, J. Chanussot, VOGTNet: Variational Optimization-Guided Two-Stage Network for Multispectral and Panchromatic Image Fusion, *IEEE Trans. Neural Netw. Learn. Syst.* (2024) 1–15.
- [123] L. Ruthotto, E. Haber, An Introduction to Deep Generative Modeling, 2021. doi:10.48550/arXiv.2103.05180. arXiv:2103.05180.
- [124] Y. Cui, P. Liu, B. Song, L. Zhao, Y. Ma, L. Chen, Reconstruction of Large-Scale Missing Data in Remote Sensing Images Using Extend-GAN, *IEEE Geosci. Remote Sens. Lett.* 21 (2024) 1–5.
- [125] T. R. Shaham, T. Dekel, T. Michaeli, SinGAN: Learning a Generative Model From a Single Natural Image, in: *Int. Conf. Comput. Vis., IEEE, Seoul, Korea (South)*, 2019, pp. 4569–4579. doi:10.1109/ICCV.2019.00467.
- [126] A. Oussidi, A. Elhassouny, Deep Generative Models: Survey, in: 2018 International Conference on Intelligent Systems and Computer Vision (ISCV), IEEE, Fez, 2018, pp. 1–8. doi:10.1109/ISACV.2018.8354080.
- [127] M. Soruri, S. M. Razavi, M. Forouzanfar, P. Colantonio, Design and Fabrication of a GaN HEMT Power Amplifier Based on Hidden Markov Model for Wireless Applications, *PLoS ONE* 18 (2023) e0285186.
- [128] W. Huang, R. Y. Da Xu, S. Jiang, X. Liang, I. Oppermann, GAN-Based Gaussian Mixture Model Responsibility Learning, in: *Int. Conf. Pattern Recog., IEEE, Milan, Italy*, 2021, pp. 3467–3474. doi:10.1109/ICPR48806.2021.9412309.
- [129] Y. Xie, L. Peng, Z. Chen, B. Yang, H. Zhang, H. Zhang, Generative Learning for Imbalanced Data Using the Gaussian Mixed Model, *Appl. Soft Comput.* 79 (2019) 439–451.
- [130] L. Manduchi, K. Pandey, R. Bamler, R. Cotterell, S. Däubener, S. Fellenz, A. Fischer, T. Gärtner, M. Kirchler, M. Kloft, Y. Li, C. Lippert, G. de Melo, E. Nalisnick, B. Ommer, R. Ranganath, M. Rudolph, K. Ullrich, G. V. den Broeck, J. E. Vogt, Y. Wang, F. Wenzel, F. Wood, S. Mandt, V. Fortuin, On the Challenges and Opportunities in Generative AI, 2024. doi:10.48550/arXiv.2403.00025. arXiv:2403.00025.
- [131] J. Correia, F. Baeta, T. Martins, Evolutionary Generative Models, in: W. Banzhaf, P. Machado, M. Zhang (Eds.), *Handbook of Evolutionary Machine Learning*, Springer Nature Singapore, Singapore, 2024, pp. 283–329. doi:10.1007/978-981-99-3814-8_10.
- [132] I. J. Goodfellow, On Distinguishability Criteria for Estimating Generative Models, 2015. doi:10.48550/arXiv.1412.6515. arXiv:1412.6515.
- [133] J. M. Graving, I. D. Couzin, VAE-SNE: a deep generative model for simultaneous dimensionality reduction and clustering, *BioRxiv* (2020) 2020–07.
- [134] H. Cao, C. Tan, Z. Gao, Y. Xu, G. Chen, P.-A. Heng, S. Z. Li, A Survey on Generative Diffusion Model, 2023. doi:10.48550/arXiv.2209.02646. arXiv:2209.02646.
- [135] F.-A. Croitoru, V. Hondru, R. T. Ionescu, M. Shah, Diffusion Models in Vision: A Survey, *IEEE Trans. Pattern Anal. Mach. Intell.* 45 (2023) 10850–10869.
- [136] P. Liu, J. Li, L. Wang, G. He, Remote sensing data fusion with generative adversarial networks: State-of-the-art methods and future research directions, *IEEE Geosci. Remote Sens. Mag.* 10 (2022) 295–328.
- [137] G. Wang, G. Dong, H. Li, L. Han, X. Tao, P. Ren, Remote Sensing Image Synthesis via Graphical Generative Adversarial Networks, in: *IGARSS 2019 - 2019 IEEE International Geoscience and Remote Sensing Symposium*, 2019, pp. 10027–10030. doi:10.1109/IGARSS.2019.8898915.
- [138] A. Radford, L. Metz, S. Chintala, Unsupervised Representation Learning with Deep Convolutional Generative Adversarial Networks (2016).

- [139] T. Karras, S. Laine, M. Aittala, J. Hellsten, J. Lehtinen, T. Aila, Analyzing and Improving the Image Quality of StyleGAN, in: IEEE Conf. Comput. Vis. Pattern Recog., IEEE, Seattle, WA, USA, 2020, pp. 8107–8116. doi:10.1109/CVPR42600.2020.00813.
- [140] A. Borji, Pros and Cons of GAN Evaluation Measures, *Comput. Vis. Image Underst* 179 (2019) 41–65.
- [141] Y.-J. Cao, L.-L. Jia, Y.-X. Chen, N. Lin, C. Yang, B. Zhang, Z. Liu, X.-X. Li, H.-H. Dai, Recent Advances of Generative Adversarial Networks in Computer Vision, *IEEE Access* 7 (2019) 14985–15006.
- [142] F. Zhan, H. Zhu, S. Lu, Spatial Fusion GAN for Image Synthesis, in: IEEE Conf. Comput. Vis. Pattern Recog., IEEE, Long Beach, CA, USA, 2019, pp. 3648–3657. doi:10.1109/CVPR.2019.00377.
- [143] E. Richardson, Y. Alaluf, O. Patashnik, Y. Nitzan, Y. Azar, S. Shapiro, D. Cohen-Or, Encoding in Style: A StyleGAN Encoder for Image-to-Image Translation, in: IEEE Conf. Comput. Vis. Pattern Recog., IEEE, Nashville, TN, USA, 2021, pp. 2287–2296. doi:10.1109/CVPR46437.2021.00232.
- [144] A. Jolicœur-Martineau, The Relativistic Discriminator: A Key Element Missing from Standard GAN, 2018. doi:10.48550/arXiv.1807.00734. arXiv:1807.00734.
- [145] W. Li, Y. He, Y. Qi, Z. Li, Y. Tang, FET-GAN: Font and Effect Transfer via K-Shot Adaptive Instance Normalization, *Proc. AAAI Conf. Artificial Intelligence* 34 (2020) 1717–1724.
- [146] A. Patil, Venkatesh, DCGAN: Deep Convolutional GAN with Attention Module for Remote View Classification, in: 2021 International Conference on Forensics, Analytics, Big Data, Security (FABS), volume 1, 2021, pp. 1–10. doi:10.1109/FABS52071.2021.9702655.
- [147] S. Ji, D. Wang, M. Luo, Generative Adversarial Network-Based Full-Space Domain Adaptation for Land Cover Classification from Multiple-Source Remote Sensing Images, *IEEE Trans. Geosci. Remote Sens.* 59 (2021) 3816–3828.
- [148] J. Song, C. Meng, S. Ermon, Denoising Diffusion Implicit Models (2022).
- [149] R. Rombach, A. Blattmann, D. Lorenz, P. Esser, B. Ommer, High-Resolution Image Synthesis with Latent Diffusion Models, in: IEEE Conf. Comput. Vis. Pattern Recog., IEEE, New Orleans, LA, USA, 2022, pp. 10674–10685. doi:10.1109/CVPR52688.2022.01042.
- [150] L. Yang, Z. Zhang, Y. Song, S. Hong, R. Xu, Y. Zhao, W. Zhang, B. Cui, M.-H. Yang, Diffusion Models: A Comprehensive Survey of Methods and Applications, 2024. doi:10.48550/arXiv.2209.00796. arXiv:2209.00796.
- [151] A. Ulhaq, N. Akhtar, Efficient Diffusion Models for Vision: A Survey, 2024. doi:10.48550/arXiv.2210.09292. arXiv:2210.09292.
- [152] S. Bengesi, H. El-Sayed, M. K. Sarker, Y. Houkpati, J. Irungu, T. Oladunni, Advancements in Generative AI: A Comprehensive Review of GANs, GPT, Autoencoders, Diffusion Model, and Transformers, *IEEE Access* 12 (2024) 69812–69837.
- [153] L. Han, Y. Zhao, H. Lv, Y. Zhang, H. Liu, G. Bi, Q. Han, Enhancing Remote Sensing Image Super-Resolution with Efficient Hybrid Conditional Diffusion Model, *Remote Sens.* 15 (2023) 3452.
- [154] Y. Liu, J. Yue, S. Xia, P. Ghamisi, W. Xie, L. Fang, Diffusion Models Meet Remote Sensing: Principles, Methods, and Perspectives, *IEEE Trans. Geosci. Remote Sens.* 62 (2024) 1–22.
- [155] N. Tasnim, I. T. Imam, M. M. A. Hashem, A Novel Multi-Module Approach to Predict Crime Based on Multivariate spatiotemporal Data Using Attention and Sequential Fusion Model, *IEEE Access* 10 (2022) 48009–48030.
- [156] S. Li, W. Li, C. Cook, C. Zhu, Y. Gao, Independently Recurrent Neural Network (IndRNN): Building A Longer and Deeper RNN, in: IEEE Conf. Comput. Vis. Pattern Recog., IEEE, Salt Lake City, UT, 2018, pp. 5457–5466. doi:10.1109/CVPR.2018.00572.
- [157] A. Sherstinsky, Fundamentals of Recurrent Neural Network (RNN) and Long Short-Term Memory (LSTM) Network, *Physica D* 404 (2020) 132306.
- [158] L. Yao, Y. Guan, An Improved LSTM Structure for Natural Language Processing, in: 2018 IEEE International Conference of Safety Produce Informatization (IICSPI), 2018, pp. 565–569. doi:10.1109/IICSPI.2018.8690387.
- [159] Chaitanya Bharathi Institute of Technology(Autonomous), K. M. Tarwani, S. Edem, Survey on Recurrent Neural Network in Natural Language Processing, *Int. J. Eng. Trends Technol.* 48 (2017) 301–304.
- [160] S. Reddy, D. Raghu, M. M. Khapra, S. Joshi, Generating Natural Language Question-Answer Pairs from a Knowledge Graph Using a RNN Based Question Generation Model, in: M. Lapata, P. Blunsom, A. Koller (Eds.), Proceedings of the 15th Conference of the European Chapter of the Association for Computational Linguistics: Volume 1, Long Papers, Association for Computational Linguistics, Valencia, Spain, 2017, pp. 376–385.
- [161] S. Kashid, K. Kumar, P. Saini, A. Dhiman, A. Negi, Bi-RNN and Bi-LSTM Based Text Classification for Amazon Reviews, in: L. Troiano, A. Vaccaro, N. Kesswani, I. Díaz Rodriguez, I. Brigui, D. Pastor-Escuredo (Eds.), Key Digital Trends in Artificial Intelligence and Robotics, volume 670, Springer International Publishing, Cham, 2023, pp. 62–72. doi:10.1007/978-3-031-30396-8_6.
- [162] C. K. Sønderby, L. Espenholt, J. Heek, M. Dehghani, A. Oliver, T. Salimans, S. Agrawal, J. Hickey, N. Kalchbrenner, MetNet: A Neural Weather Model for Precipitation Forecasting, 2020. doi:10.48550/arXiv.2003.12140. arXiv:2003.12140.
- [163] W. Fang, L. Pang, V. S. Sheng, Q. Wang, STUNNER: Radar Echo Extrapolation Model Based on Spatiotemporal Fusion Neural Network, *IEEE Trans. Geosci. Remote Sens.* 61 (2023) 1–14.
- [164] R. S. Sutton, B. Tanner, Temporal-Difference Networks, in: Advances in Neural Information Processing Systems, volume 17, MIT Press, 2004.
- [165] B. Ivanovic, M. Pavone, The Trajectron: Probabilistic Multi-Agent Trajectory Modeling With Dynamic Spatiotemporal Graphs, in: Int. Conf. Comput. Vis., IEEE, Seoul, Korea (South), 2019, pp. 2375–2384. doi:10.1109/ICCV.2019.00246.
- [166] T. Zhang, S.-Y. Liew, H.-F. Ng, D. Qin, H. C. Lee, H. Zhao, D. Wang, GraphAT Net: A Deep Learning Approach Combining TrajGRU and Graph Attention for Accurate Cumulonimbus Distribution Prediction, *Atmosphere* 14 (2023) 1506.
- [167] Y. Wang, M. Long, J. Wang, Z. Gao, P. S. Yu, PredRNN: Recurrent Neural Networks for Predictive Learning Using Spatiotemporal LSTMs, in: Adv. Neural Inf. Process. Syst., volume 30, Curran Associates, Inc., 2017.
- [168] S. Hochreiter, J. Schmidhuber, Long Short-Term Memory, *Neural Computation* 9 (1997) 1735–1780.
- [169] Y. Li, R. Chen, Y. Zhang, M. Zhang, L. Chen, Multi-Label Remote Sensing Image Scene Classification by Combining a Convolutional Neural Network and a Graph Neural Network, *Remote Sens.* 12 (2020) 4003.
- [170] X. Gao, J. Haworth, I. Ilyankou, X. Zhang, T. Cheng, S. Law, H. Chen, SMA-Hyper: Spatiotemporal Multi-View Fusion Hypergraph Learning for Traffic Accident Prediction, 2024. doi:10.48550/arXiv.2407.17642. arXiv:2407.17642.
- [171] T.-Y. Lin, P. Dollár, R. Girshick, K. He, B. Hariharan, S. Belongie, Feature Pyramid Networks for Object Detection, in: IEEE Conf. Comput. Vis. Pattern Recog., IEEE, Honolulu, HI, 2017, pp. 936–944. doi:10.1109/CVPR.2017.106.
- [172] R. Yan, J. Liao, J. Yang, W. Sun, M. Nong, F. Li, Multi-Hour and Multi-Site Air Quality Index Forecasting in Beijing Using CNN, LSTM, CNN-LSTM, and Spatiotemporal Clustering, *Expert Syst. Appl.* 169 (2021) 114513.
- [173] Z. Zhang, Z. Huang, Z. Hu, X. Zhao, W. Wang, Z. Liu, J. Zhang, S. J. Qin, H. Zhao, MLPST: MLP Is All You Need for spatiotemporal Prediction, 2023. doi:10.48550/arXiv.2309.13363. arXiv:2309.13363.
- [174] X. Zhang, L. Xie, S. Li, F. Lei, L. Cao, X. Li, Wuhan Dataset: A High-Resolution Dataset of Spatiotemporal Fusion for Remote Sensing Images, *IEEE Geosci. Remote Sens. Lett.* 21 (2024) 1–5.
- [175] V. C. Radeloff, D. P. Roy, M. A. Wulder, M. Anderson, B. Cook, C. J. Crawford, M. Friedl, F. Gao, N. Gorelick, M. Hansen, S. Healey, P. Hostert, G. Hulley, J. L. Huntington, D. M. Johnson, C. Neigh, A. Lyapustin, L. Lyburner, N. Pahlevan, J.-F. Pekel, T. A. Scambos, C. Schaaf, P. Strobl, C. E. Woodcock, H. K. Zhang, Z. Zhu, Need

- and Vision for Global Medium-Resolution Landsat and Sentinel-2 Data Products, *Remote Sens. Environ.* 300 (2024) 113918.
- [176] X. Li, Q. Peng, Y. Zheng, S. Lin, B. He, Y. Qiu, J. Chen, Y. Chen, W. Yuan, Incorporating Environmental Variables Into Spatiotemporal Fusion Model to Reconstruct High-Quality Vegetation Index Data, *IEEE Trans. Geosci. Remote Sens.* 62 (2024) 1–12.
- [177] F. Lyu, Z. Yang, C. Diao, S. Wang, Multistream STGAN: A Spatiotemporal Image Fusion Model With Improved Temporal Transferability, *IEEE J. Sel. Top. Appl. Earth Obs. Remote Sens.* 18 (2025) 1562–1576.
- [178] R. Wu, X. Wen, L. Yuan, H. Xu, DASFTOT: Dual Attention Spatiotemporal Fused Transformer for Object Tracking, *Knowl.-Based Syst.* 256 (2022) 109897.
- [179] P. Wang, M. Huang, S. Shi, B. Huang, B. Zhou, G. Xu, L. Wang, H. Leung, Landsat-8 and Sentinel-2 Image Fusion Based on Multiscale Smoothing-Sharpening Filter, *IEEE J. Sel. Top. Appl. Earth Obs. Remote Sens.* 17 (2024) 17957–17970.
- [180] L. T. Luppino, M. A. Hansen, M. Kampffmeyer, F. M. Bianchi, G. Moser, R. Jenssen, S. N. Anfinsen, Code-Aligned Autoencoders for Unsupervised Change Detection in Multimodal Remote Sensing Images, *IEEE Trans. Neural Netw. Learn. Syst.* 35 (2024) 60–72.
- [181] X. Su, J. Li, Z. Hua, Transformer-Based Regression Network for Pansharpening Remote Sensing Images, *IEEE Trans. Geosci. Remote Sens.* 60 (2022) 1–23.
- [182] Y. Song, H. Zhang, H. Huang, L. Zhang, Remote Sensing Image Spatiotemporal Fusion via a Generative Adversarial Network With One Prior Image Pair, *IEEE Trans. Geosci. Remote Sens.* 60 (2022) 1–17.
- [183] Y. Cui, P. Liu, Y. Ma, L. Chen, M. Xu, X. Guo, Pixel-Wise Ensembled Masked Autoencoder for Multispectral Pansharpening, *IEEE Trans. Geosci. Remote Sens.* 62 (2024) 1–22.
- [184] C. Shang, X. Li, Z. Yin, X. Li, L. Wang, Y. Zhang, Y. Du, F. Ling, Spatiotemporal Reflectance Fusion Using a Generative Adversarial Network, *IEEE Trans. Geosci. Remote Sens.* 60 (2022) 1–15.
- [185] Z. Ao, Y. Sun, Q. Xin, Constructing 10-m NDVI Time Series From Landsat 8 and Sentinel 2 Images Using Convolutional Neural Networks, *IEEE Geosci. Remote Sens. Lett.* 18 (2021) 1461–1465.
- [186] J. Chen, L. Wang, R. Feng, P. Liu, W. Han, X. Chen, CycleGAN-STF: Spatiotemporal Fusion via CycleGAN-Based Image Generation, *IEEE Trans. Geosci. Remote Sens.* 59 (2021) 5851–5865.
- [187] D. Jia, C. Cheng, C. Song, S. Shen, L. Ning, T. Zhang, A Hybrid Deep Learning-Based Spatiotemporal Fusion Method for Combining Satellite Images with Different Resolutions, *Remote Sens.* 13 (2021) 645.
- [188] Y. Ma, J. Wei, W. Tang, R. Tang, Explicit and Stepwise Models for Spatiotemporal Fusion of Remote Sensing Images with Deep Neural Networks, *Int. J. Appl. Earth Obs. Geoinf.* 105 (2021) 102611.
- [189] A. Krizhevsky, I. Sutskever, G. E. Hinton, Imagenet classification with deep convolutional neural networks, *Commun. ACM* 60 (2017) 84–90.
- [190] T.-Y. Lin, M. Maire, S. Belongie, J. Hays, P. Perona, D. Ramanan, P. Dollár, C. L. Zitnick, Microsoft coco: Common objects in context, in: D. Fleet, T. Pajdla, B. Schiele, T. Tuytelaars (Eds.), *Eur. Conf. Comput. Vis.*, Springer International Publishing, Cham, 2014, pp. 740–755.
- [191] B. Huang, Y. Zhao, Research status and prospect of spatiotemporal fusion of multi-source satellite remote sensing imagery, *Acta Geod. Cartogr. Sin.* (2017).
- [192] M. Sdraka, I. Papoutsis, B. Psomas, K. Vlachos, K. Ioannidis, K. Karantzas, I. Gialampoukidis, S. Vrochidis, Deep Learning for Downscaling Remote Sensing Images: Fusion and Super-Resolution, *IEEE Geosci. Remote Sens. Mag.* 10 (2022) 202–255.
- [193] D. Niu, H. Che, C. Shi, Z. Zang, H. Wang, X. Chen, Q. Huang, A Heterogeneous Spatiotemporal Attention Fusion Prediction Network for Precipitation Nowcasting, *IEEE J. Sel. Top. Appl. Earth Obs. Remote Sens.* 16 (2023) 8286–8296.
- [194] H. Shen, M. Jiang, J. Li, C. Zhou, Q. Yuan, L. Zhang, Coupling Model-Driven and Data-Driven Methods for Remote Sensing Image Restoration and Fusion, *IEEE Geosci. Remote Sens. Mag.* 10 (2022) 231–249.
- [195] Q. Yang, C. Jin, T. Li, Q. Yuan, H. Shen, L. Zhang, Research Progress and Challenges of Data-Driven Quantitative Remote Sensing, *National Remote Sensing Bulletin* 26 (2022) 268–285.
- [196] Z. Wang, Y. Ma, Y. Zhang, Review of Pixel-Level Remote Sensing Image Fusion Based on Deep Learning, *Inf. Fusion.* 90 (2023) 36–58.
- [197] X. X. Zhu, D. Tuia, L. Mou, G.-S. Xia, L. Zhang, F. Xu, F. Fraundorfer, Deep Learning in Remote Sensing: A Review, *IEEE Geosci. Remote Sens. Mag.* 5 (2017) 8–36.
- [198] X. Cheng, Y. Zheng, J. Zhang, Z. Yang, Multitask Multisource Deep Correlation Filter for Remote Sensing Data Fusion, *IEEE J. Sel. Top. Appl. Earth Obs. Remote Sens.* 13 (2020) 3723–3734.
- [199] J. M. Leiva-Murillo, L. Gomez-Chova, G. Camps-Valls, Multitask Remote Sensing Data Classification, *IEEE Trans. Geosci. Remote Sens.* 51 (2013) 151–161.
- [200] A. Xiao, W. Xuan, J. Wang, J. Huang, D. Tao, S. Lu, N. Yokoya, Foundation Models for Remote Sensing and Earth Observation: A Survey, 2024. doi:10.48550/arXiv.2410.16602. arXiv:2410.16602.
- [201] Y. Cong, S. Khanna, C. Meng, P. Liu, E. Rozi, Y. He, M. Burke, D. Lobell, S. Ermon, SatMAE: Pre-training Transformers for Temporal and Multi-Spectral Satellite Imagery, *NeurIPS* 35 (2022) 197–211.
- [202] C. J. Reed, R. Gupta, S. Li, S. Brockman, C. Funk, B. Clipp, K. Keutzer, S. Candido, M. Uyttendaele, T. Darrell, Scale-MAE: A Scale-Aware Masked Autoencoder for Multiscale Geospatial Representation Learning, in: *Int. Conf. Comput. Vis.*, IEEE, Paris, France, 2023, pp. 4065–4076. doi:10.1109/ICCV51070.2023.00378.
- [203] A. Fuller, K. Millard, J. Green, CROMA: Remote Sensing Representations with Contrastive Radar-Optical Masked Autoencoders, *NeurIPS* 36 (2023) 5506–5538.
- [204] S. Khanna, P. Liu, L. Zhou, C. Meng, R. Rombach, M. Burke, D. Lobell, S. Ermon, DiffusionSat: A Generative Foundation Model for Satellite Imagery, 2024. doi:10.48550/arXiv.2312.03606. arXiv:2312.03606.